J Paleolimnol (2006)
DOI 10.1007/s10933-006-9002-0

ORIGINAL PAPER

Records of environmental and climatic changes during the late Holocene from Svalbard: palaeolimnology of Kongressvatnet

Piero Guilizzoni · Aldo Marchetto · Andrea Lami · Achim Brauer · Luigi Vigliotti · Simona Musazzi · Leonardo Langone · Marina Manca · Federico Lucchini · Natale Calanchi · Enrico Dinelli · Alceo Mordenti

Received: 13 May 2005 / Accepted: 25 March 2006

Abstract A multi-core, multidisciplinary palaeolimnological study of the partially varved sediment of a deep, meromictic, arctic lake, Kongressvatnet (Svalbard, Western Spitsbergen), provides a record of environmental and climatic changes during last ca. 1800 years. The chronology of sedimentation was established using several dating techniques (^{137}Cs, ^{210}Pb, varve counts, palaeomagnetic correlation). A multiproxy record of palaeolimnological variability was compiled based on sedimentation rates, magnetic properties, varve thickness, organic matter, geochemistry, pigments from algal and photosynthetic bacteria, mineralogy and biological assemblages (diatoms, Cladocera). The major features recognised in our master core K99-3 include a shift in sediment source and supply (magnetic measurements, geochemistry) probably caused by glaciological changes in the catchment around 38–32 cm core depth (AD 700–820). Additional environmental changes are inferred at 20–18, 8–4.5 and 3–2 cm (AD ca. 1160–1255; 1715–1880; 1940–1963, respectively). During the past ca. 120 years a prominent sedimentological change from brownish-grey, partly laminated silt-clay (varves) to black organic-rich deposits was observed. From AD 1350 to AD1880 the sediment is comprised of a continuous sequence of varves, whereas the earlier sediments are mostly homogeneous with only a few short intercalated laminated sections between AD 860 and 1350. Sedimentation and accumulation rates increased during the last 30 years (modern warming). Pigment concentrations are very low in the lower ca. 32 cm of the core (AD 820) probably because of the high turbidity high energy environment. The high sulphur content in the uppermost 32 cm of sediment has given rise to two horizontally stratified populations of sulphur anaerobic photosynthetic bacteria, as inferred from their specific carotenoids. These bacteria populations are much more abundant during the Little Ice Age (LIA) than during warmer periods (e.g., during the Medieval Warm Period and 20th century). Diatoms are lacking from the core base up to 18 cm (ca. AD 1255); at this level, species indicative of mesotrophic water are present, whereas from 17 cm to the top of the core, oligotrophic taxa such as *Staurosira construens/S. pinnata* complex dominate, indicating

P. Guilizzoni (✉) · A. Marchetto · A. Lami · S. Musazzi · M. Manca
CNR—Istituto per lo Studio degli Ecosistemi (ex Istituto Italiano di Idrobiologia), Largo V. Tonolli 50, 28922 Verbania Pallanza, Italy
e-mail: p.guilizzoni@ise.cnr.it

L. Vigliotti · L. Langone
CNR ISMAR, Istituto Scienza del Mare, Via P. Gobetti 101, 40129 Bologna, Italy

A. Brauer
GeoForschungsZentrum, D-14473 Potsdam, Germany

F. Lucchini · N. Calanchi · E. Dinelli · A. Mordenti
Dipartimento Scienze della Terra, Università di Bologna, Piazza Porta S. Donato, 40126 Bologna, Italy

extended ice coverage and more oligotrophic waters during the LIA. The concentration of Cladocera subfossil remains (dominated by *Chydorus*) are relatively high in the deepest sections (54–32 cm), whereas the upper 32 cm are characterized by a very low concentration of remains, possibly because of the strongly anoxic conditions, and in this upper sediment section rotifer resting eggs become prevalent. We interpret these changes as responses to climate forcing through its impact on glacial melt water, lake ice cover duration and mainly redox conditions in deep water. The observed changes suggest that at least some of our recorded changes may parallel the Greenland Ice core, although our study added more details about the inferred climatic changes. Further aspects are discussed, such as catchment processes, glacial activity, duration of the Medieval Warm Period, the Little Ice Age, local human activity, and limnology.

Keywords Diatoms · Pigments · Cladocera · Sediment · Geochemistry · Varves · Magnetic properties · Climate · Spitsbergen

Introduction

Polar and mountain ecosystems are highly vulnerable to climate changes and human impact (Lotter et al. 2002). They play a key role in global change (Lami et al. 2000a and 2000b) and are thought to play an important role in a number of positive feedback cycles. Responses to global warming are predicted to be greatest in these environments, and to occur there first. The best known palaeoclimatic archives from the Arctic are the Greenland ice cores (e.g., Grootes et al. 1993), but for the Holocene these ice cores show only little variability. This is different from lake sediment records that show major environmental changes throughout the Holocene (e.g., Hardy et al. 1998; Willemse and Törnqvist 1999; Wagner et al. 2000; Nowaczyk et al. 2001; Andreev et al. 2003, 2004; Kremenetski et al. 2004; Smith et al. 2004), and especially over the last ca. 150 years (Antoniades et al. 2005; Karst-Riddoch et al. 2005). Lakes on Svalbard have been shown to be particularly sensitive to environmental changes (Birks et al. 2004a, b).

Kongressvatnet was selected for this multy-proxy study because it is thought to be a sensitive ecosystem with respect to atmospheric pollution and climate variability. The short growing season, despite a relatively high mid-summer productivity, ensures low annual production compared to temperate lakes. Additionally, chemical weathering rates are climate-dependent factors that regulate, in part, the nutrient supply to lakes (Smol et al. 1991). The simple trophic structure makes lakes from Svalbard well-suited for studying lake-catchment-climate interactions.

Evaluation of natural and anthropogenic forcing on lake biota requires long-term records of physical, chemical and biological proxies. Specifically, this study aims to detect ecosystem responses to low-amplitude, natural climatic changes, as well as to the impacts from pollution, either local or remote (e.g., Rose et al. 2004). At Svalbard, for some pollutants, concentrations during the winter can reach values as high as those for rural areas in North and central Europe (Rahn 1981).

Our project has two major objectives:

1. To provide high resolution multiproxy palaeoclimate records for the late Holocene using a large variety of geochemical and biological indicators;
2. To assess the temporal effect of environmental and climatic change on lake ecosystem structure and processes.

This paper presents the results obtained from Kongressvatnet and focuses on the analyses of stratigraphic variations in physical, chemical and biological proxy records. Among these, pigments derived from algae and from anaerobic photosynthetic bacteria have proven to be a reliable proxy of modern algal biomass, and also allow the reconstruction of past algal community changes (Leavitt and Hodgson 2001). Diatom assemblages and invertebrate fossil remains (cladocerans) allow quantification of past changes in pH, temperature, nutrient enrichment, dissolved oxygen and salinity (Anderson 2000; Battarbee 2000; Korhola et al. 2005). Chironomid remains in Lake Kongressvatnet were very few, not enough for a stratigraphic study, and are thus not reported here. In addition, biostratigraphical records based on these proxy indicators can also be used to reconstruct ecosystem responses to environmental variations, especially with respect to aquatic productivity, and lake catchment surface processes

which, if responding synchronously, are likely to reflect regional climatic variations (Smol et al. 2005).

Catchment processes (erosion, remobilisation of littoral sediments) and chemical weathering can be described from sedimentological and geochemical data. Micro-facies analyses is required to prove the seasonal nature of the macroscopically observed laminations in order to establish a varve chronology, and additional information on extreme precipitation events can be obtained from the identification of turbidites. Further non-quantitative grain-size and mineralogical data might indicate changes in the sediment source as well as depositional processes.

Magnetic properties, including magnetic susceptibility, and lithological information have been applied for core correlation and for tracing changes in the source of detrital sediment fluxes while palaeomagnetic secular variations have been used as the sole dating tool for the pre-1900 sediments of Kongressvatnet (see below).

The collection of several cores, which were correlated by magnetic susceptibility and lithology, was necessary to provide enough sediment for the high number of proxies that were analysed and the sample time resolution.

The study area

Kongressvatnet (78°01′ N, 13°58′ E; Figs. 1, 2) is a small (0.82 km^2), deep (Z_{max} = 37 m) and meromictic lake (Bøyum and Kjensmo 1970) near Barentsburg (Norden Skiöld Land) in the inner part of the valley Kongressdalen, with an elevation of 94 m a.s.l. Two mountain ranges reaching elevations from 450 to 675 m shelter the lake surface from winds. At the end of April 1999, we obtained sediment cores from 37 m water depth from the ice-covered lake. According to our field portable eco-sonar measurements (SCUBAPRO, PDS-2), this is the maximum depth of the lake in spring time; however, Bøyum and Kjensmo (1970) measured in the summer of 1968 a greater depth of ca. 52 m. It is common that in winter water level decreases and lake fluctuations can be the result of subsurface drainage towards the valley of Linnédalen (Fig. 2) forming thick icings (sheets of ice formed below springs in winter) on the valley floor (J. Mangerud, personal communication). The lake is ice covered for about 9–10 months.

From the ionic composition of the water, Kongressvatnet is a characteristic sulphate lake. The ionic composition of different water depths at the date of coring is shown in Table 1. Concentrations of reactive and total phosphorus are very low (<3 μg l^{-1}). Ca and Mg dominate among the cations, and sulphate is the dominating anion in Kongressvatnet. The high content of Ca, Mg and SO_4 are derived from the rocks of the catchment, particularly from layers of gypsum (Bøyum and Kjensmo 1970). The pH was alkaline (pH = ca 8.0).

Four small streams drain into the lake, and two of them drain an area that contains small glaciers. The water of one of these rivulets, running through different rocks, originates from three mineral springs rich in hydrogen sulphide and is responsible for the meromictic stability of this lake (Geological map 1:500000, Norsk Polarinstitutt, Dallmann 1993). From this map the catchment area consists of Carboniferous-Permian limestone and gypsum (migmatite complex is located west to the lake). Only a small portion of the catchment is partially covered by glaciers, and today the glacier does not drain into the lake. More information about the lake water and landforms is given by Bøyum and Kjensmo (1970, 1980). The postglacial upper marine limit is between 65 and 78 m (Svendsen et al. 1987) so no marine incursion occurred at Kongressvatnet.

The Svalbard Archipelago is not pristine, and is affected by atmospheric contaminants (Rose et al. 2004). Several investigations have shown that the Svalbard atmosphere in winter is heavily loaded with a variety of anthropogenic pollutants which include sulphates and sulphur dioxide, heavy metals (e.g., Pb, Cu, Zn and Ni), and organic gases (e.g., alkani) (Simões and Zagorodnov 2001 and references therein).

The vegetation cover is patchy, and consists of herbs and mosses. Trees are absent and tundra vegetation prevails. Vascular plants are sparse and the number of species is low. Permafrost is found throughout the area.

The average temperature of the coldest month (February) at Ny-Ålesund is ca. −15 °C (−12 °C at Isfjord Radio) whereas the average July temperature range from ca. + 5 °C (Isfjord Radio) to 6.5 °C (at Longyearbyen). The relatively mild climate of the western coast is due to the influence of the Gulf Stream, here the so-called Norwegian Current. Its climate can thus be termed arctic-oceanic. The

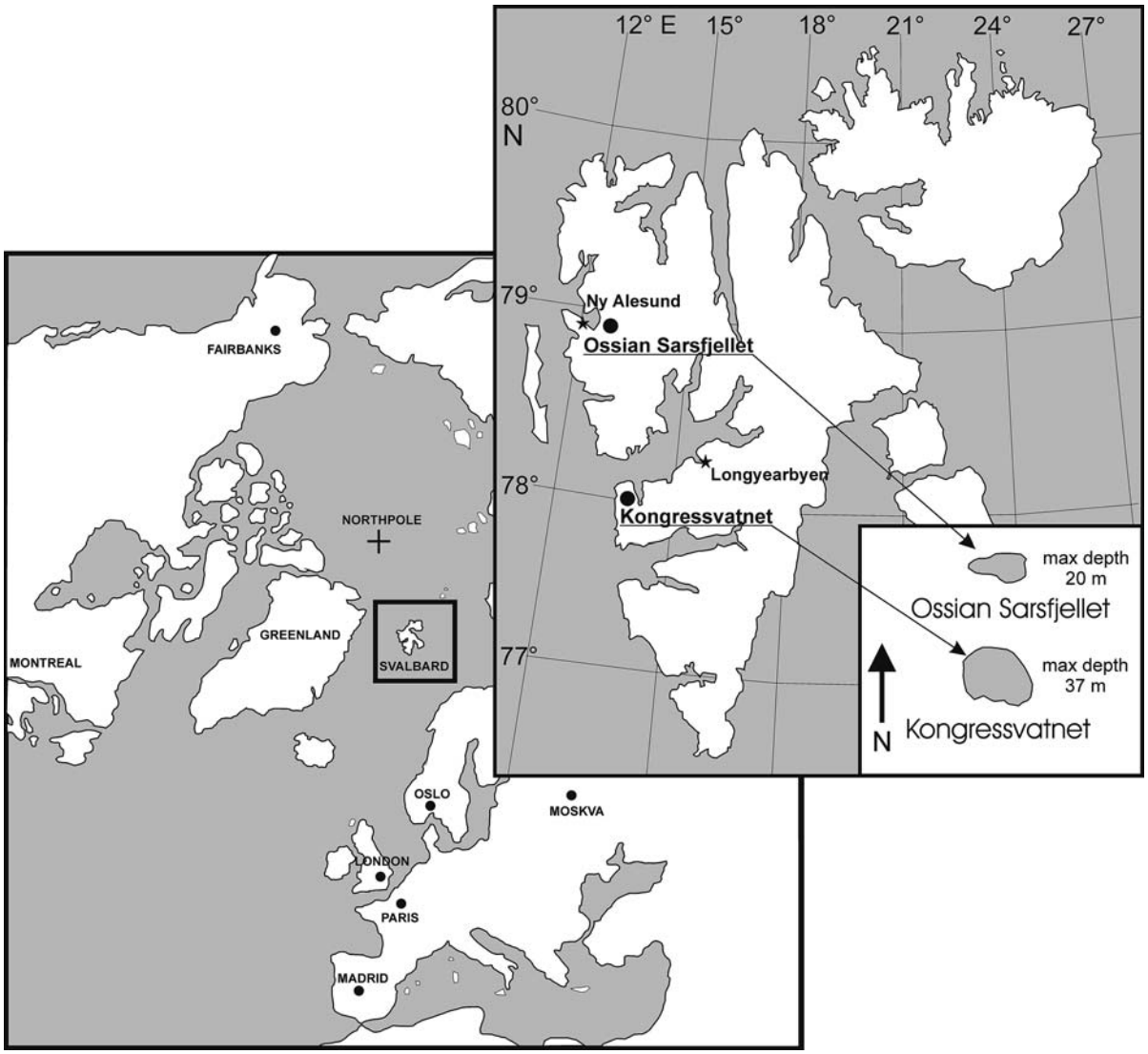

Fig. 1 Location map showing Kongressvatnet and another investigated lake (L. Ossian Sarsfjellet) mentioned in the text

longest temperature record from Svalbard, covering the period 1912–1996, is reported by van de Wal et al. (2002): mean annual temperature over this period is −6.3 °C. Large fluctuations in temperature values are evident during the 20th Century. The mean annual precipitation of 370 mm year^{-1} in Ny-Ålesund (measurements from 1975 to 1989) decreases to ca. 200–300 mm in inland areas. Although the 20th century climate data reported here and in the sections below are from different sources, the general trend of variations is similar and consistent, as summarized by Hanssen-Bauer and Førland (1998).

In addition, details on the climate of Svalbard during the Holocene (Birks 1991) and of the past four centuries are reported in Birks et al. (2004a). Past climate changes are reflected by regional changes in glacier extent. For example, the Linnébreen glacier, located ca. 5 km south of Kongressvatnet, started to form 4000–5000 years ago as a local reflection of neo-glaciation. The Holocene maximum extension of this glacier has been reported to occur during the 'Little Ice Age' (LIA) (Svendsen and Mangerud 1997). Ice-core data from Svalbard suggest a duration of the LIA from AD1550–1920 (references in Birks

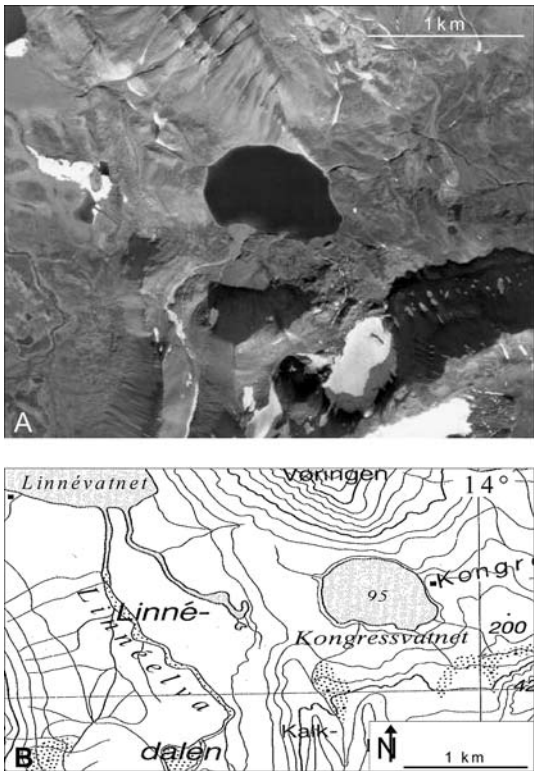

Fig. 2 Aerial photograph of Kongressvatnet taken on 19 August 1969 with a view from the north-west (**A**) (photo S90 2482 obtained from (**A**). Werner and the Norwegian Polar Institute). A map of the lake with respect to Lake Linnévatnet is also shown (Svalbard 1:100 000 Isfjorden, Norsk Polarinstitutt, Oslo 1989) (**B**)

et al. 2004a). Other ice-core records suggest a two-phase development with cold periods between AD 1200–1500 and AD 1700–1900. Local moraines probably of this period (Fig. 2) are also present in the catchment of Kongressvatnet indicating that climate is the major factor for regional changes in glacier extent (Werner 1993).

Methods

Sampling and analyses

In April 1999, three sediment cores (K99-2, K99-3, K99-5; 50.5 cm, 54.5 cm, 48 cm, respectively), from the deepest part of Kongressvatnet, were taken from ice using a gravity corer and were sub-sampled in the laboratory at contiguous 0.5-cm intervals to obtain an average sample resolution of 13 years per 0.5 cm for the last ca. 150 years (ca. 9 years for the last 45 years; see the chronology section below). All the chemical and biological analyses were performed on K99-3 (master core, Fig. 3), whereas cores K99-2 and K99-5 were sampled for the magnetic and macrofacies studies, respectively.

Magnetic parameters

Whole-core magnetic susceptibility was measured in core K99-2 using a Bartington MS IB instrument along each core prior to cutting the cores. In addition, a more complete magnetic characterisation of the lake sediments has been accomplished: the core was sampled for magnetic measurements by inserting plastic cubic boxes (8 cc) in the sediments. The natural remanent magnetization (NRM), vectors recorded in the sediments were measured using a F.I.T. spinner magnetometer. Stepwise alternating-field (AF) cleaning was carried out using a Molspin demagnetizer with peak AF fields between 0 and 60 mT.

Mass-specific magnetic susceptibility was measured by using a Bartington MS2 susceptibility meter.

Isothermal remanent magnetization (IRM) up to 1 Tesla (T) was imparted to a subset of samples by using an ASC IM-30 pulse magnetizer. Back field DC demagnetisation to 0.3 T was used to calculate the S-ratio parameter in order to determine the magnetic properties of the minerals.

Mineralogy and geochemistry

Mineral composition was determined on core K99-3 by X-Ray diffraction (XRD) (Philips PW 1710 spectrometer with Cu tube) on powder pressed into alumina holders to prevent any strong orientation of sheet-silicates. Major and trace elements analyses were performed by X-Ray Fluorescence (XRF) (Philips PW1480) on sediment powder pellets, applying the matrix corrections methods of Franzini et al. (1972, 1975), Leoni and Saitta (1976) and Leoni et al. (1982). The estimated precision and accuracy for trace element determinations are better than 5% except for those elements at 10 ppm and lower (10–15%); the detection limit for the most trace elements is 3 ppm (Leoni and Saitta 1976). Scanning electron microscopy (SEM) and Energy Dispersive

Table 1 Temperature, pH and water chemistry characteristics of Kongressvatnet

Depth (m)	T (°C)	pH	Conductivity (20 °C μS m^{-1})	T. Alk. (meq l^{-1})	Cl (mg l^{-1})	SO_4 (mg l^{-1})	N–NO_3 (mg l^{-1})	N–NH_4 (mg l^{-1})	TN (mg l^{-1})
3	1.3	8.1	639	1.03	4.5	327	0.02	0.02	0.06
15	1.6	7.8	605	1.10	4.4	357	0.03	0.01	0.05
30	1.8	7.9	687	1.05	4.2	357	0.06	0.01	0.12
32	1.8	8.1	669	1.03	4.0	334	0.05	0.00	0.08
37	1.8	8.1	682	1.06	4.5	370	0.09	0.00	0.11
Depth (m)	Ca (mg l^{-1})	Mg (mg l^{-1})	Na (mg l^{-1})	K (mg l^{-1})	Si (mg l^{-1})				
3	118	23.4	3.6	0.4	0.7				
15	128	26.5	3.5	0.3	0.8				
30	125	25.6	3.2	0.3	0.9				
32	120	23.6	3.4	0.4	0.6				
37	129	27.5	3.6	0.3	0.7				

T. Alk. = Total alkalinity; TN = Total nitrogen

Spectrometer (EDS) observations were carried out using a scanning electron microscope Philips 515 equipped with an energy-dispersive spectrometer EDAX 9100.

Micro-facies analyses

A continuous series of large-scale thin sections (120 × 35 mm) with an overlap of 2 cm each were prepared from core K99-5 for microscopic analyses. Eight mm thick sediment slices were freeze-dried and subsequently impregnated with a transparent two-component resin (Araldite 2020). After fixing the impregnated sediment blocks on glass slides, thin slices were cut and polished down to a thickness of 20 μm. Analyses were carried out with a petrographic microscope (Carl Zeiss Axiophot) with magnifications ranging from 12.5× to 400×. For measurement of varve and detrital layer thickness 100× magnification was used. Thin-section images were obtained with a digital camera (Carl Zeiss Axiocam) using the software Carl Zeiss Axiovision 2.0.

Loss-on-ignition

Water content, organic matter and carbonate content were determined on core K99-3 by drying 5–6 g of wet sediment at a temperature of 80 °C (for 36–48 h to constant weight), 450 °C and 950 °C (Santisteban et al. 2004). An accurate and stable weight loss was achieved after 4 h of burning ash sediment at 950 °C, whereas to estimate the organic content, dry samples were burned at 450 °C overnight (ca. 12 h).

Pigments

On samples from core K99-3, photosynthetic pigments were extracted using 90% acetone, overnight (16 h) in the dark, under N_2 (Lami et al. 2000b). The extract obtained was used both to quantify the chlorophylls and their derivatives (Chlorophyll Derivatives units, CD) and total carotenoids (TC) by spectrophotometer (Lami et al. 1994). Using a Beckman Gold System (Lami et al. 2000b), individual carotenoids were detected by Reversed Phase High Performance Liquid Chromatography (RP-HPLC). Carotenoids analysed were restricted to total algal community (β-carotene), cryptophytes (alloxanthin), siliceous algae (diatoms, chrysophytes) and some dinoflagellates (fucoxanthin), dinoflagellates (peridinin), chlorophytes (lutein), cyanobacteria (echinenone), and purple (okenone) and green sulphur bacteria (isorenieratene). Carotenoid concentrations are expressed in nanomoles per gram of organic matter (nmol g_{OM}^{-1}), to avoid the problem of dilution with clastic materials entering from the catchment, and chlorophyll derivatives in units per gram of organic matter (U g_{OM}^{-1}).

Diatoms

On samples from core K99-3, diatoms were prepared using standard H_2O_2–HCl digestion (Renberg 1990) and mounted in Naphrax. On each slide, a minimum of 500 diatom valves was enumerated by light microscopy, and taxonomic features confirmed by scanning electron microscopy procedures. Diatom

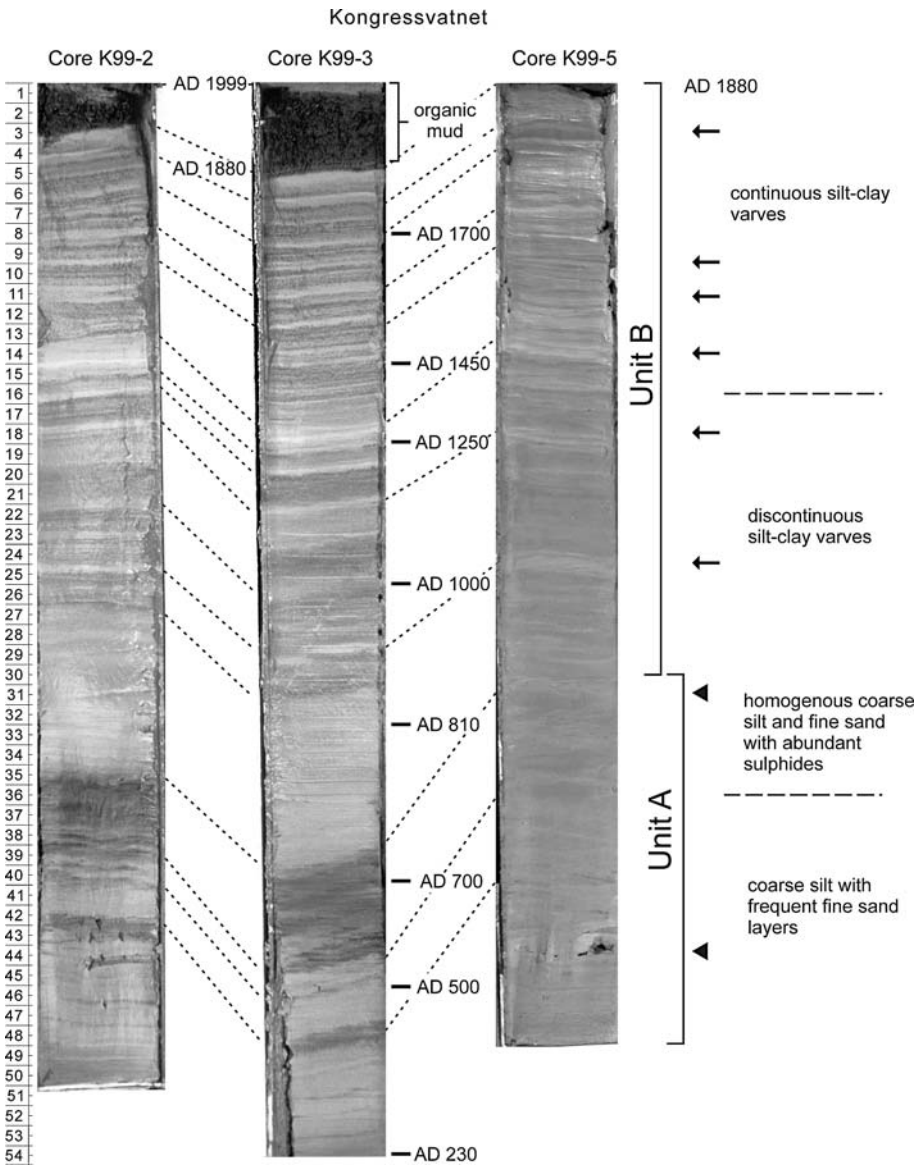

Fig. 3 Photograph, lithological description and core correlation of sediment cores from Kongressvatnet. Ages are derived from a chronological model based on different dating methods (see text). Arrows indicate prominent graded silt layers; triangles indicate drop stone layer. Two main lithological units (A and B) including two sub-units each are also described. Core length in centimetre

taxonomy followed Krammer and Lange-Bertalot (1986–1991). The abundance of taxa was expressed as relative percentages.

Cladocera

To analyse fossil Cladocera, wet sediment (about 1 g) from core K99-3 was deflocculated in warm 10% KOH for 2 h and then digested in HCl 10% (Frey 1986). The concentrate of the remains was then transferred into 5% formalin. We counted up to 200 remains per sample (Hann and Karrow 1993), identifying them to genus/species and, when possible, morphotype level, after Frey (1958) and Hofmann (1978). Following Frey (1986), we converted the counts into population estimates for each taxon and expressed fossil concentrations as number of exuviae per g d.w.$^{-1}$ (No. g d.wt.$^{-1}$). Following Pielou (1977),

we also calculated species richness (S) and the Shannon-Weaver diversity index (H') of chydorids. This is calculated by:

$$\text{diversity}, H = -\sum_{i=1}^{S} \text{Pi} \ln \text{Pi} \quad (1)$$

where S is the total number of species in the community and Pi the number of individuals of the ith species. As required, the value of the index depends on both the species richness and the evenness (equitability) with which individuals are distributed among the species. Rarefaction analysis was used to eliminate the effect of different sample size.

Dating

Because of the need for sufficient material for all the analyses, the time scale for the Kongressvatnet sediment record was established using multiple dating techniques applied on three different cores (K99-2, K99-3 and K99-5). However, these cores have been easily correlated by means of magnetic susceptibility and lithology (Fig. 4). Then, an age/depth model (see below) has been derived from a combination both of independent dates on a given core and of correlations between cores.

The top part of core K99-3 was dated using the short-lived radionuclides ^{210}Pb and ^{137}Cs. ^{210}Pb ($t_{1/2}$ = 22.26 years) and ^{137}Cs ($t_{1/2}$ = 30.2 years) were counted via gamma spectrometry using an Ortec HPGe GMX-20195 (gamma-x type) coaxial intrinsic germanium detector (Frignani et al. 1991; Giordani et al. 1992). A Constant Rate of Supply (CRS) model was applied to the activity depth-profiles of excess ^{210}Pb (Appleby and Oldfield 1978, 1983). ^{137}Cs peaks were attributed to the Chernobyl accident in 1986 and to maximum global fallout reflecting the tests of atomic bombs (1963). In many ice cores of Svalbard glaciers, the Chernobyl layer was detected (Pourchet et al. 1995). However, the highest concentration of ^{137}Cs was shown to be representative of the maximum fallout of ^{137}Cs from atmospheric nuclear tests (1963) (Pinglot et al. 1999; Appleby 2004).

For sediment older than ca. 100 years, two independent approaches were applied: (1) measurement of palaeomagnetic direction in the sediments from core K99-2 to obtain a secular variation curve used to match varve-dated sediment record from Finland and the French archaeomagnetic master curve; (2) varve counting and varve-based sedimentation rate estimation have been applied to core K99-5. Clastic varves are almost continuously preserved between 5 and 30 cm depth (Fig. 3), whereas in the lower part non-laminated intervals prevail. For these non-laminated intervals, sedimentation rates have been calculated on the basis of varve thickness data from the adjacent varved intervals. An assumption for such calculations was that sediment composition and grain-size was similar for the varved and non-laminated intervals.

AMS radiocarbon dating of nine bulk samples (Van de Graaff Laboratory, University of Utrecht, NL

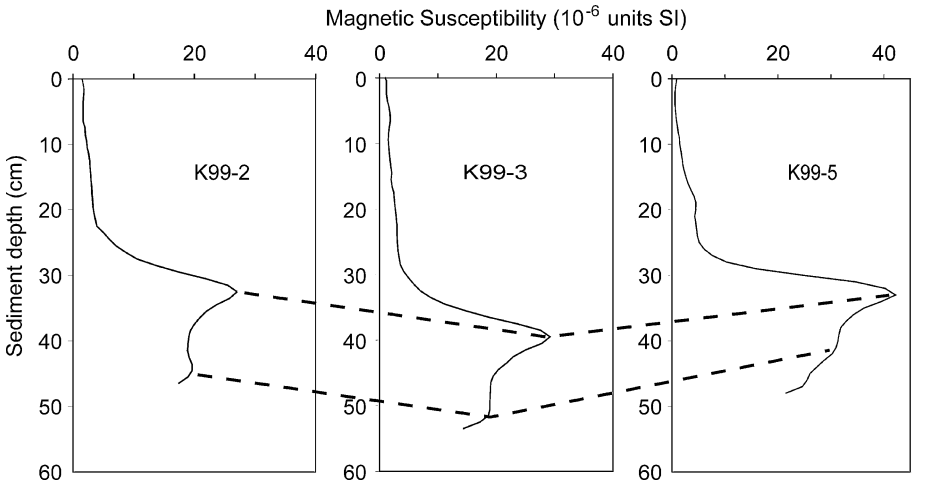

Fig. 4 Core correlation based on susceptibility scans among cores from Kongressvatnet

and Center for Accelerator Mass Spectrometry, L. Livermore National Laboratory, USA) resulted in ages that were clearly too old (>9000 years BP) due to finely dispersed microscopic coal particles and reservoir effects (detrital calcite). A similar contamination was observed in the sediment of the nearby Linnévatnet (Snyder et al. 1994). Unfortunately, macroscopic terrestrial plant remains were lacking in our cores.

Results and discussion

Core correlation

Core correlation of all three cores (K99-2, K99-3, K99-5) by lithostratigraphy and magnetic susceptibility (Figs. 3, 4) revealed that some cores are slightly more expanded than others (Figs. 3, 4). The upper part of the profile is characterised by low magnetic susceptibility; however, this increases significantly below 32 cm depth (Fig. 4). In core K99-5, the topmost 3–4.5 cm dark organic layer visible in cores K99-2 and K99-3, is missing (see below). Comparing the depths among cores of specific peaks and lithological markers demonstrates variations of up to 7 cm.

Sediment setting

The sediment record from Lake Kongressvatnet is characterized by a prominent change at about 4.5 cm depth from brownish-grey, partly laminated detrital sediments to a black organic-rich layer on the very top. This black layer has been recovered in cores K99-2 and K99-3 (Fig. 3). The detrital sediments are described from core K99-5 using a continuous series of thin sections. These sediments are mainly composed of carbonate minerals (dolomite, calcite) with only a smaller fraction of quartz and clay minerals reflecting the geology of the catchment basin. Dispersed pyrite framboids and fine coal particles are ubiquitous. The detrital sediment sequence can be further sub-divided into two units (A and B, see Fig. 3), which distinctly differ in micro-facies and grain size. The transition between these units appears to be gradual at about 30–32 cm. The upper sediment Unit (B) consists of finely laminated silt and clay deposits. Laminated intervals are intercalated with homogeneous sections from about 15–30 cm depths and continuous from 15 cm depths almost until the boundary to the black organic surface sediments.

Microscopic analyses clearly demonstrate a regular two sub-layer depositional system. Basal silt-sized, sometimes slightly graded layers gradually pass into a thin clay layer on top (Fig. 5a). Thicker graded layers, interpreted as turbidites, are occasionally intercalated (Fig. 5b). The basal layers of these turbidites often include diatom fragments of *Campylodiscus* sp. indicating reworked material from the littoral zone. The lower Unit (A) is mostly homogeneous with few intercalated short intervals of a coarser lamination that consists of couplets of fine sand and mixed silt-clay (Fig. 5c) below 35 cm depths (core K99-5). Plant remains (Fig. 5d) and iron sulphides (Fig. 5e) often related to decomposed plant fragments are more common than in the upper part. Intervals with enriched sulphide particles can be recognized by a blackish sediment colour, for example, at 32–40 cm depths (core K99-2; Fig. 3). Abundant isolated sand-to pebble-sized grains within fine-grained matrix sediments (Fig. 5f) are interpreted as drop stones. Two discrete layers of ice rafted detritus appear at 30.5 cm and 43–44 cm depths (Fig. 3).

The origin of the sandy lamination in the Unit A obviously reflects higher energetic depositional environment but its origin remains unclear. In contrast, there are convincing sedimentological analogues for the fine lamination in Unit B in recent annual laminations from a lake in the Canadian Arctic (Zolitschka 1996). This supports their interpretation as true clastic varves as typically occurring in proglacial and periglacial lakes (e.g., Brauer et al. 1994). The common origin of these varves is differential speed of settling depending on grain size. During the short summers, detrital particles were transported with snow and glacier melt water into the lake. The larger silt particles immediately sank to the lake bottom whereas clay particles remained in suspension until extreme quiet water conditions under frozen lake conditions developed in winter. A further proof of this seasonal deposition are drop stones, which were released from drift ice during the ice break-up and settled on top of the winter clay layers and, thereby, slightly deformed them (Fig. 5a). These clastic varves are the dominant type of fine laminations at Kongressvatnet (>95% of all couplets). Their

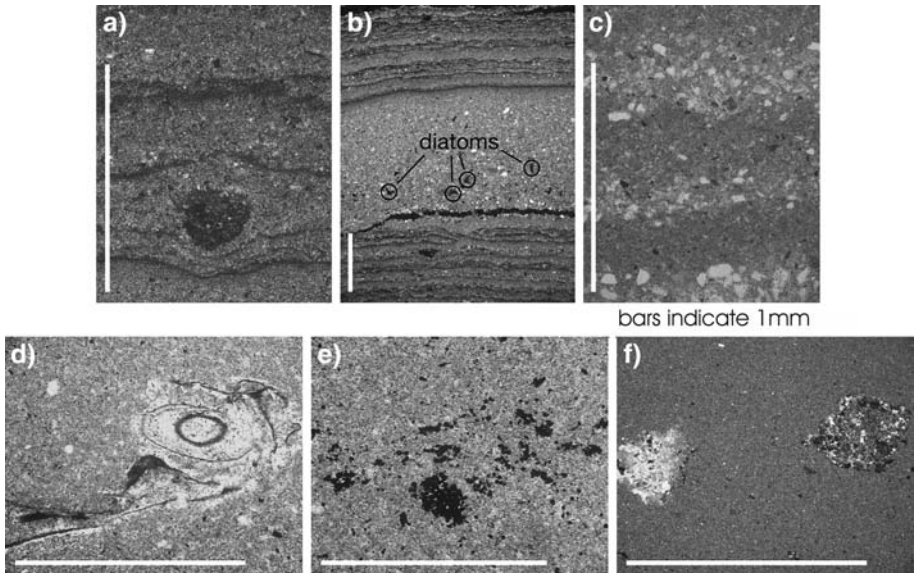

Fig. 5 Thin section images (**a**–**f**) from core K99-5 sediments. Except (**c**) and (**d**) all images are made with cross-polarized light. (**a**) silt/clay couplets interpreted as clastic varves; one dropstone-like sand grain has deformed the winter clay layer of a varve, 3 cm depth; (**b**) graded detrital layer interpreted as extreme runoff event at 2.5 cm depth. Embedded in the coarse basal layer are diatom fragments of *Campylodiscus noricus* (marked by black circles); (**c**) coarser lamination from the lower unit consisting of fine sand/silt couplets, 42 cm depth; (**d**) unspecified plant fragment, 21 cm depth; (**e**) spots of greigite framboid accumulations (black dots); (**f**) two dropstone-like sand grains in fine-grained homogeneous matrix; dropstone layer at 30 cm depth

formation required sufficient detrital sediment fluxes and, probably more importantly, stable freezing conditions in winter. Variations in varve thickness (Fig. 6) are interpreted as a summer temperature proxy (Leemann and Niessen 1994; Brauer 2004) since the rate of ice and snow melt that controls the sediment yield largely depends on summer temperatures.

Magnetic parameters

Rock magnetic parameters measured in core K99-2 (X, SIRM, S-Ratio, SIRM/X; Fig. 7) indicate that a different magnetic content characterizes the core sediments. Low values of concentration related parameters X and SIRM occur in the uppermost 25 cm of core (30 cm in master core K99-3), indicating that a minor magnetic content characterise this interval. These parameters increase below 30 cm of depth suggesting a higher magnetic content for the bottom of the core. The coincident increase in the S-ratio indicates that ferrimagnetic minerals (magnetite type) dominate in this part of the core whereas minerals with higher coercivity (hematite or goethite type) occur at the top of the core. The two peaks in SIRM/X, coinciding with those in SIRM and high 'S' values, are the result of greigite (Fe_2S_4) formation. This ferromagnetic iron sulphide is magnetically characterised by high values of interparametric ratio SIRM/X (Snowball 1991) and usually it forms in fresh/brackish water where Fe and S are sufficiently abundant and conditions are sufficiently reducing for pyritization to begin—i.e. it is part of the solid solution series that eventually results in pyrite. This result suggests that two different sources characterize the magnetic supply as a possible consequence of two processes: (1) meltwater or glacier emplacement occurring in the catchment, (2) dissolution of magnetite. According to the magnetic curves the evidence may be against a simple reductive diagenesis (dissolution) and more for a sediment source shift tied to the level of glacial melt/or particle size. Base on the proposed chronology (see below), this change occurred in the 7th–8th century corresponding to a period of significant climatic deterioration known as the ''Dark Ages Cold Period'' (Berglund 2003).

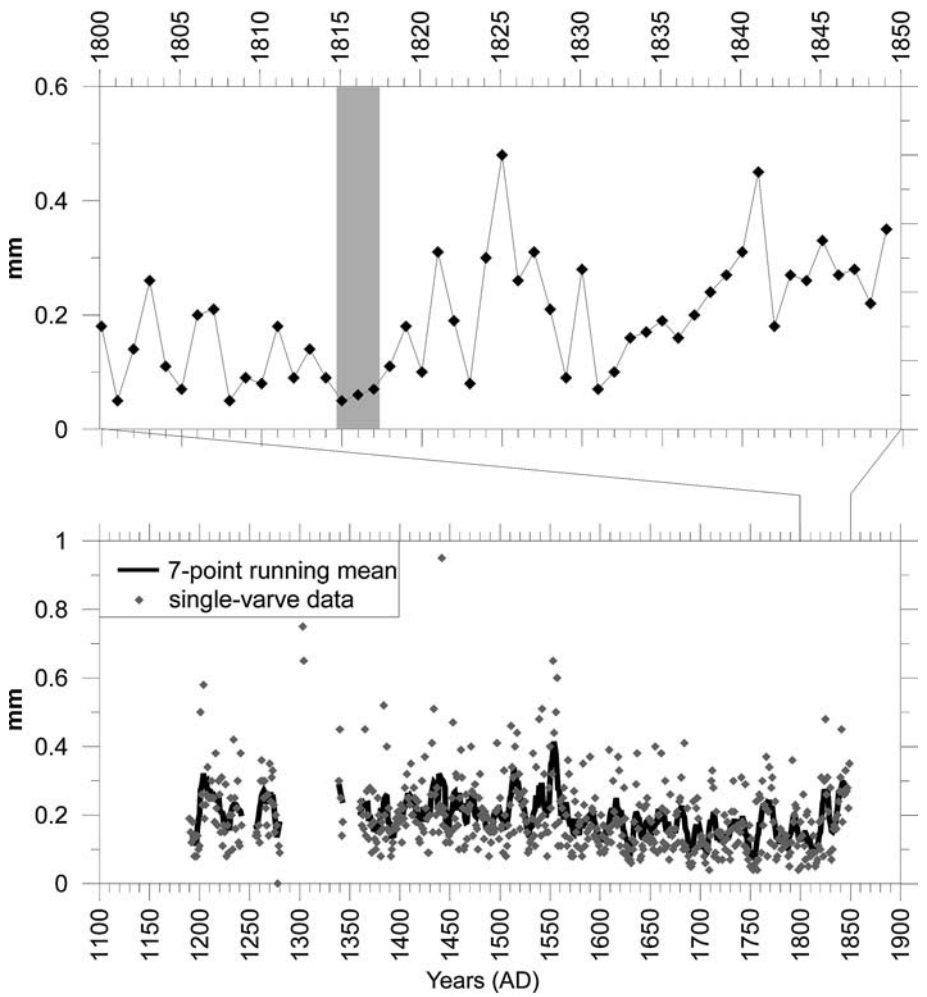

Fig. 6 Varve thickness variations measured from core K99-5 (0–15 cm depths) for the varved part of the sediments from Kongressvatnet. In intervals without thickness data, varve boundaries were not distinct enough for reliable measurements. Upper panel: zoom-out of the varve thickness data from AD 1800 to 1850. *Note*: minimum in varve thickness between AD 1815 and 1817

Chronology

In general, dating of predominantly clastic sediment records is not a trivial task due to the limited number of dating techniques and their uncertainties. Therefore, a multiple dating approach has been applied for the sediment record from Lake Kongressvatnet in order to achieve the best possible age model. Dating methods include (1) radiometric dating for the uppermost part of the record, (2) varve dating and varve-based sedimentation rate estimates, and, (3) correlation of palaeomagnetic data with a varve-dated lake sediment record from Finland and French archaeometric data.

Recent chronology (last ca. 150 years). The uppermost part of the sediment core K99-3 was dated using short-lived radionuclides (^{137}Cs and ^{210}Pb), which enable us to calculate the sediment accumulation rates for approximately the last 50–150 years. (Fig. 8).

The ^{137}Cs, an artificial radionuclide supplied by fallout from atomic weapon testing and releases from power plants, was detectable in the upper 2.5–3.0 cm of the sediment core (Fig. 8a). If this represents 1954

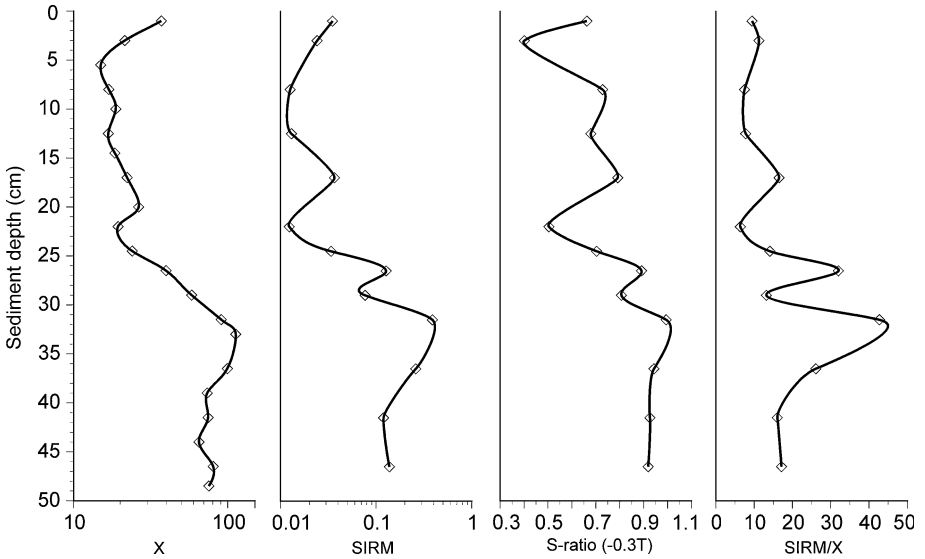

Fig. 7 Downcore (Kongressvatnet, core K99-2) profiles of magnetic properties. X (10^{-9} m^3 kg^{-1}), SIRM (10^{-5} A m^2 kg^{-1}), SIRM/X (A m^{-1})

(onset of experiment weapons), a mean sedimentation rate of 0.61 mm $year^{-1}$ is calculated for the last 45 years. However, a well-apparent peak of ^{137}Cs was measured at 1.5–2 cm depth. Assuming this peak as related to the 1963 fallout caesium (Pinglot et al. 1999), the resulting sedimentation rate is 0.49 mm $year^{-1}$. The Chernobyl signal in ice and sediment cores of the Arctic is much less evident compared with the clear maximum in 1962–63 (Pinglot et al. 1999 and references therein).

The ^{210}Pb chronology based on a comprehensive CRS approach enables calculation of sedimentation rates for the last century (Fig. 8b, c). ^{210}Pb activities fluctuate throughout the sediment cores and cease at 4.5 cm depth. Assuming negligible biological mixing (justified by lake meromixis conditions), accumulation rates have been calculated according to Appleby and Oldfield (1978, 1983). An average sedimentation rate based on the CRS M-90 (depth where the ^{210}Pb integral reaches 90% divided by 74 years) gave a value of 0.47 mm $year^{-1}$ (0.024 g cm^{-2} $year^{-1}$), which is in good agreement with the estimate from the ^{137}Cs-peck of the 1963 fallout. Applying the mass sediment accumulation rate (0.024 g cm^{-2} $year^{-1}$), it reveals an extrapolated age of AD 1881 for the lithological change (4.75 cm, 2.82 g cm^{-2}). This age is similar to observations in nearby Lakes Ossian (AD 1869; Musazzi 2005) and Lake Lillevatnet (AD 1889) (unpublished data).

Pre-20th century chronology

The chronology for the record beyond radiometric dating has been established on the parallel cores K99-5 (varve chronology) and K99-2 (palaeomagnetic correlation; Fig. 9). The dates have been transferred to the master core K99-3 through detailed core correlation based on marker layers (Fig. 3) and prominent features in magnetic susceptibility (Fig. 4). The distinct lithological change at 4.5 cm sediment depth marks the anchor point where the varve chronology has been connected to the radiometric dating. Thus varve counts start at AD 1880 as obtained from ^{210}Pb and ^{137}Cs dating. Varve counts are continuous only in the uppermost part. The section below is only partly varved, still allowing varve-based sedimentation rate estimates. For the lower, non-varved part of the record, simple extrapolation has been applied. Thus, an age of ca. AD 230 has been estimated for the base of the study core (Fig. 10).

From 5 to 14 cm, 490 continuous varves have been counted. In the lower part of the record, another 125 varves have been identified in seven individual sections, each containing between 5 and 52 varves. Thickness measurements of these varves have been used for sedimentation rate calculations. Sedimentation rates vary between 0.23 and 0.30 mm $year^{-1}$, with maximum values reached between 23 and 30 cm depth, a section characterized by slightly coarser

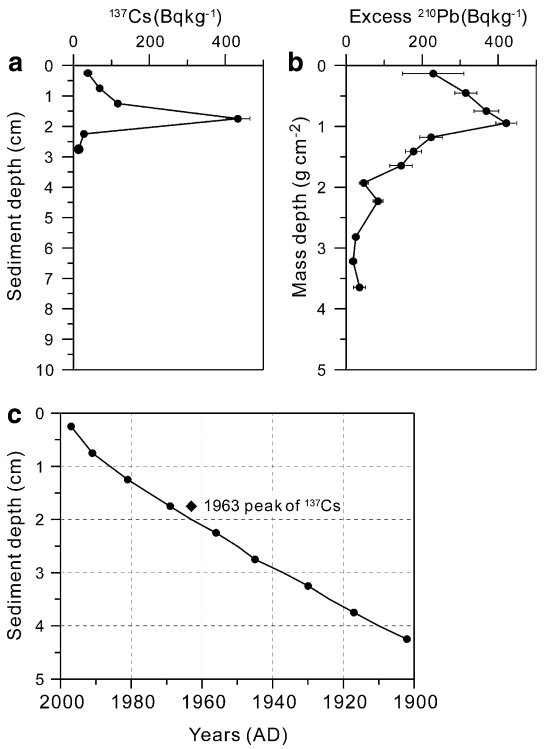

Fig. 8 Activity/depth profiles of short-lived radionuclides measured from core K99-3 collected in Kongressvatnet: (**a**) ^{137}Cs plotted against sediment depth (cm); (**b**) excess ^{210}Pb versus cumulative dry mass (g cm^{-2}); (**c**) plot of ages versus sediment depths based on calculations of the CRS model applied to excess ^{210}Pb data; the depth of the 1963 ^{137}Cs peak is also shown, which is in good agreement with CRS results

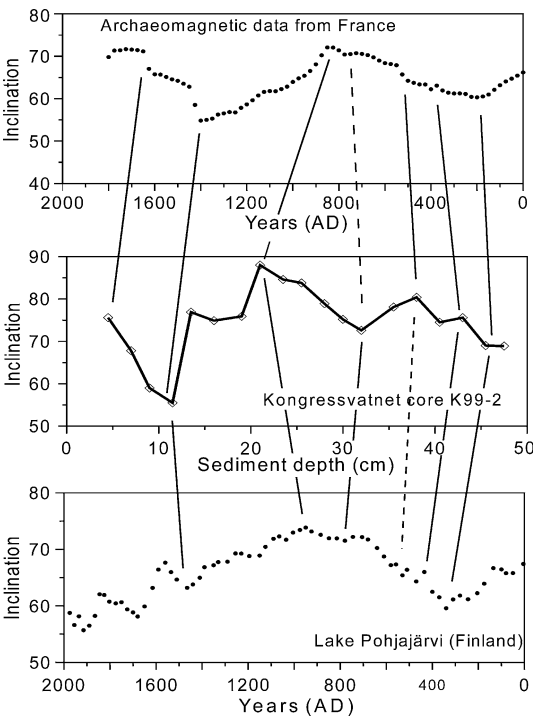

Fig. 9 Inclination profile of core K99-2 of Kongressvatnet and comparison with dated master curves from western Europe and Finland. Dashed line: uncertain boundary

grained varves. Below 39 cm depth (AD 700) no varves are preserved. The upper part of the varve chronology might be supported by a short and distinct drop in varve thickness for the years ca. AD 1815–1817 (Fig. 6). Accepting the interpretation of varve thickness as proxy for summer temperature, the low values measured for these three years could reflect a short-term cooling related to the Tambora eruption in AD 1815. A series of cold summers has been reported during that period also from tree ring studies (Briffa et al. 1998).

The varve-based age model is confirmed by correlating six distinct features in inclination with palaeomagnetic results from the varve-dated Lake Pohjajärvi in Finland (Saarinen 1999) and archaeomagnetic data from France (Daly and Le Goff 1996) (Fig. 10). Although magnetic declination exhibits some scattering either due to sampling, or as an artefact of the steep inclination (70°–85°), as expected for the high latitude of the site, the inclination profile shows the same pattern as known from other well-dated records (Fig. 9). In particular the low inclination values from 8 to 12 cm depth compare well with the prominent minimum in master curves from Western Europe which occurred in the 14th–15th centuries AD (Daly and Le Goff 1996). Steep inclinations between 20–25 cm depth could represent a peak (γ) dated elsewhere at ca 1000 to 1200 year BP (Thouveny and Williamson 1991; Saarinen 1999). The significant correlation of features of secular variations between lacustrine sediments from Spitsbergen and European mid-latitude records has been already recognised by Løvlie et al. (1991).

The resulting age for the base of the record is about the same for the extrapolated varve chronology and the correlation with the Pohjajärvi record and about 100 years older as derived from the correlation with the French archaeomagnetic data. This difference is within the assumed uncertainty in all applied dating approaches.

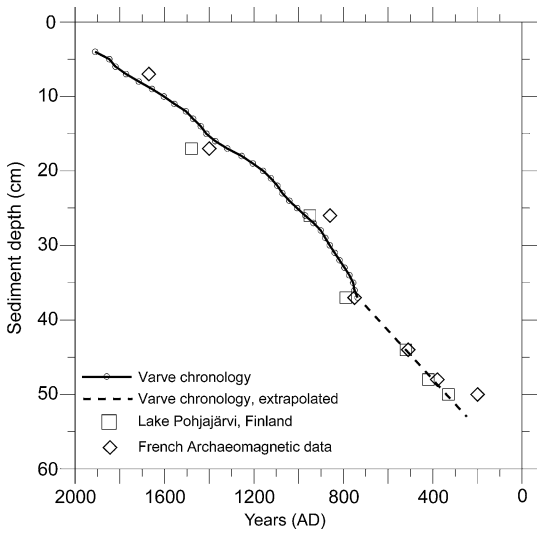

Fig. 10 Depth-age plot for core K99-3. Varve counts obtained from core K99-5 have been transferred to K99-3 for each cm (as indicated by the open circles) based on the distinct sedimentological marker layers (see Fig. 3). The start of the varve count at 4.5 cm reflects the lithological boundary between the topmost black organic layer and the predominantly clastic sediments below. The date for this point is AD1880 according to ^{137}Cs and ^{210}Pb dating (see Fig. 8). The lower part of the varve-based chronology (dashed line) has been extrapolated because in this section no varves are preserved. The varve dating is confirmed by correlation of prominent features in inclination with the archaeomagnetic record from France (open rhombs) and a palaeomagnetic lake record from Finland (open squares)

Mineralogy and inorganic geochemistry

The main mineral phases of core K99-3 identified by XRD are: dolomite, quartz, calcite (cc/dol 0–0.2), clay minerals (muscovite/illite, chlorite) and feldspars. The high content of carbonates originates from the erosion of dolomite and limestone of the Carboniferous Nordenskoldbreen Formation in the catchment area of Kongressvatnet; the silicate fraction derives from the Mesozoic siliciclastic rocks outcropping at the eastern side of the lake. Variable carbonates/silicates and calcite/dolomite ratios occur throughout the core (Fig. 11), and this suggests some changes in the sediment supply through time.

The chemical features of the Kongressvatnet sediments display the carbonate signature, but the wide variations in SiO_2 (21–37%), Al_2O_3 (5–9%), MgO (10–15%), CaO (13–23%) and CO_2 (20–30%) contents provide further evidence for the mineralogical variations observed.

Among minor and trace elements, the wide range of S content (650–10600 ppm) appears remarkable. According to the downcore behaviour of the major and trace elements, three main groups of elements can be identified (Fig. 12). One group (MgO, CaO, CO_2, MnO) is related to carbonates; a second large group is split into two sub-groups,one including SiO_2, Al_2O_3, K_2O among major elements, and Rb, V and Ba among trace elements, refers to aluminosilicate fraction, and one including Zr, Y, Nb, La and Th refers to coarse-grained resistant heavy minerals; the third group includes elements (e.g. Fe_2O_3, Ni, Cr, Co, Zn, S) with undefined sources.

The chemical depth profiles of the elements carried by aluminosilicates are complementary to those of carbonates (Fig. 12), and allow the identification of four main zones characterized by different silicate/carbonates ratios. Zone I is distinguished by the low contents of SiO_2, Al_2O_3 and Rb, and high of MgO and CaO; zone II is identified by the increase of SiO_2, Al_2O_3 and Rb, and the decrease of MgO and CaO; zone III matches zone 1 but Fe content increases upcore; finally, zone IV is characterized by the sharp increase of SiO_2, Al_2O_3 and Rb followed by an irregular decrease. On the whole, from the core bottom to about 40 cm (ca. AD 230–643) and from 20 to 10 cm (AD 1159–1600) the sediment is more carbonate rich than in the intermediate (40 to 20 cm) and upper (10 to 3 cm) zone (AD 1600–1940). However, if we consider the profiles of Ca/Mg and of (Zr+Rb)/Sr ratios a layer rich of carbonates occurs also in the intermediate zone from 29 to 26 cm.

The profile of S is characterized upwards by a sharp increase in S content. The first and second zones from the bottom overlap rather well the lowest ones defined by the carbonate/silicate ratios, whereas zone III includes sediments from 18 to 6 cm. Zone IV shows a S decline. Although the increase of S content appears linked to the aluminosilicate fraction, the sulphur profile above 16 cm differs from those of aluminosilicate elements (e.g., Al_2O_3, K_2O) and fits very well to that of iron. This suggests that the sulphur in the sediment may be carried by iron sulphides. Sulphides are usually associated to the siliciclastic fraction of the sediments (thin section clearly show the formation of pyrite (FeS) or greigite (Fe_3S_4) around plant fragments too). However, in this core sulphur appears enriched also in the 20–10 cm range depth rich in carbonates. This enrichment could

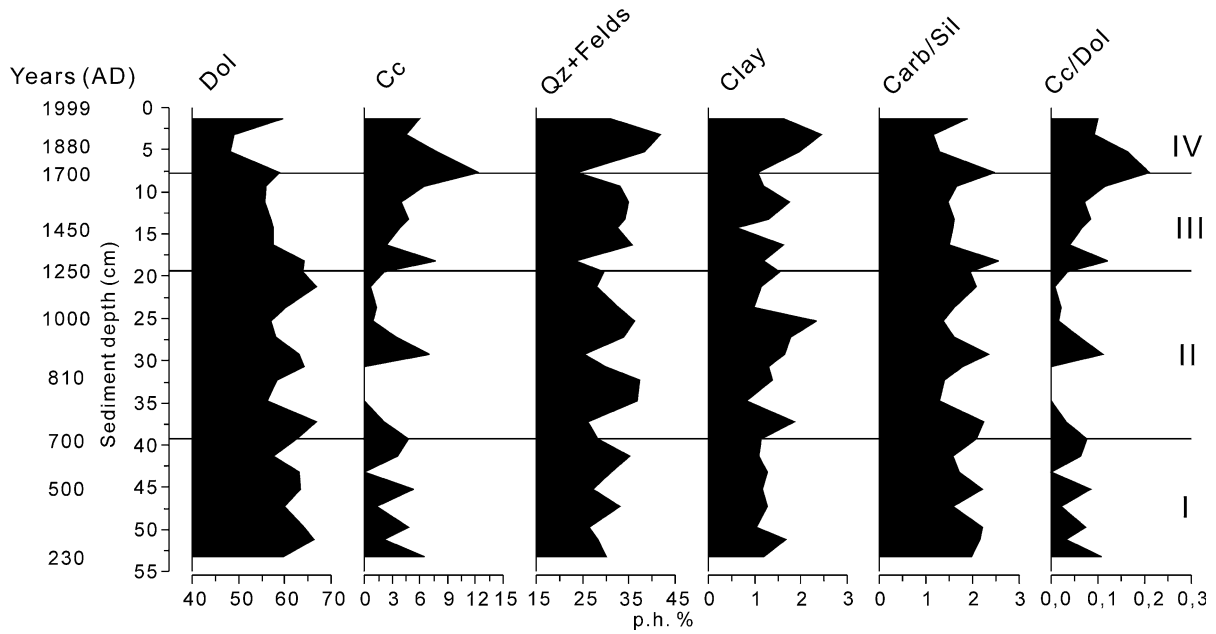

Fig. 11 XRD semiquantitative estimate of the main mineral phases (p.h.% = relative peak high per cent) of the Kongressvatnet sediments (core K99-3). Dol: dolomite; Cc: calcite; Qz + Felds: sum of quartz and feldspars; Clay: sum of clay minerals; Carb/Sil: carbonates/silicates ratio; CC/Dol: calcite/dolomite ratio. The horizontal lines distinguish four main zones with distinctive geochemistry (see text). Chronology is based on multiple dating (Fig. 10)

be related to a higher sulphide content, but we could not exclude the presence of sulphates in the sediment. In fact, gypsum layers occur in the Kongressvatnet drainage area inter-bedded to the Carboniferous dolomite and limestone (Dallmann 1993). They are considered responsible for both the high sulphate content of the lake water and the precipitates of calcium sulphate found in the rivulet bed entering the lake (Bøyum and Kjensmo 1970). Since the presence in the sediment of iron sulphide, or instead of calcium sulphate, has different significance as regards the redox conditions at the lake bottom, the identification of the S carrier is crucial. Indeed SEM-EDS observations allowed us to identify many spheroidal particles (3–5 μm in size) of iron suphides (framboidal pyrite confirmed in thin sections; Fig. 13), spread out among carbonate and silicate grains, but no sulphate particles. Accordingly, the degree of pyritisation (DOP = pyrite Fe/total Fe; Berner 1970), a reliable index of palaeo-oxygenation, was calculated assuming that all sulphur is present as pyrite (Jones and Manning 1994). Reducing conditions during the phase of high S content are also indicated by the high concentrations of photosynthetic sulphur bacteria pigments (see below).

Dry weight, loss on ignition, organic carbon, total carbon, total nitrogen

The dry weight profile shows several peaks that are related to changes in sediment texture and external input of minerals (erosion e.g. at 4.5 cm, 17.5 cm; Fig. 14). Between 54.5 cm and 35 cm the water content is unusually low (ca. 30% w.w.) and high susceptibility values are measured (Fig. 4).

Terrestrial vegetation is extremely rare and the organic compounds in the sediments are believed to be almost entirely derived from within lake productivity. The sedimentary organic matter, C and N were different and variable through time (Fig. 14). These biogeochemical parameters have low values (LOI = 3–6% d.w.; total C = ca. 7–8%; org. N = 0.1–0.2%).

LOI, which is highly correlated with organic nitrogen, increase upwards (max values at 1–2 cm). A relatively steady increase is observed from 37 cm

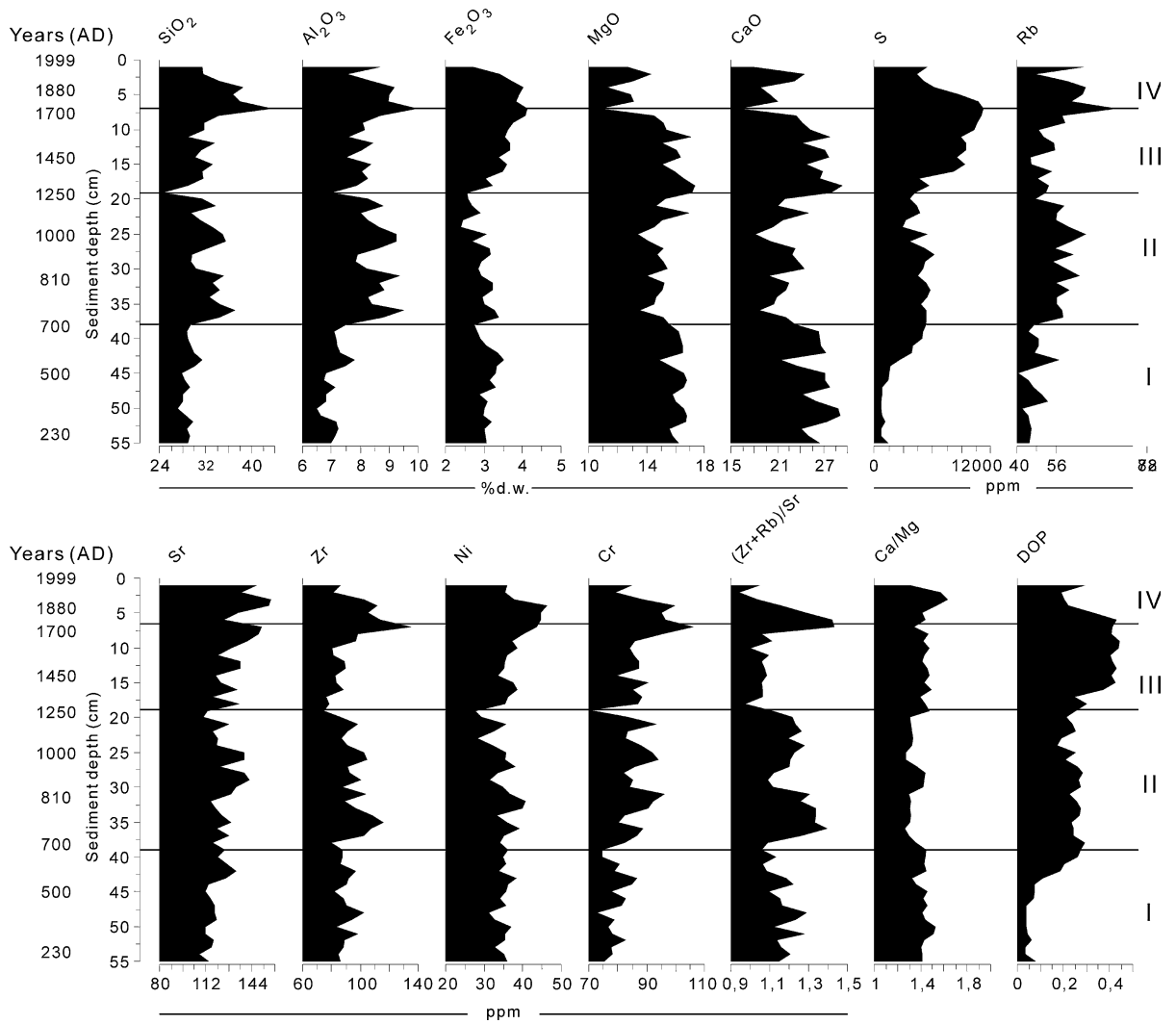

Fig. 12 Depth profiles of selected major and trace elements and of some geochemical indices representative of the main sediment components in the Kongressvatnet sediments (core K99-3). The (Zr + Rb)/Sr ratio reflects the balance between siliciclastic (Zr and Rb rich) and carbonate (Sr rich) components (Dypvik and Harris 2001); Ca/Mg ratio supports both the calcite vs. dolomite variations and those of carbonates vs. silicates; DOP is the degree of pyritization (DOP = pyrite Fe/total Fe; Berner 1970)

upwards. Low values are at ca. 7 cm (AD 1772) and at the bottom of the core.

Algal and bacterial fossil pigments

Total chlorophyll derivatives (CD) and total carotenoids (TC) are indicators of algal abundance, whereas single carotenoid remains are used as signatures for specific algal taxa.

CD, TC, and in general all sedimentary pigments have very low concentrations in the lower ca. 30 cm of the core (zone I; Fig. 15). CD and TC profiles are very similar to ß-carotene, a pigment produced by all algal taxa, and were more abundant in the past, in particular between 18 cm and 8 cm (zone IV), than recent periods with minimum values from 25 to17 cm. An abrupt change is shown at 8 cm. Fucoxanthin (diatoms, siliceous algae) is present only in the topmost samples and in zone II. Other carotenoids more resistant to decomposition such as echinenone (cyanobacteria) and lutein, a characteristic pigment of green plants, are absent or very much reduced in zone

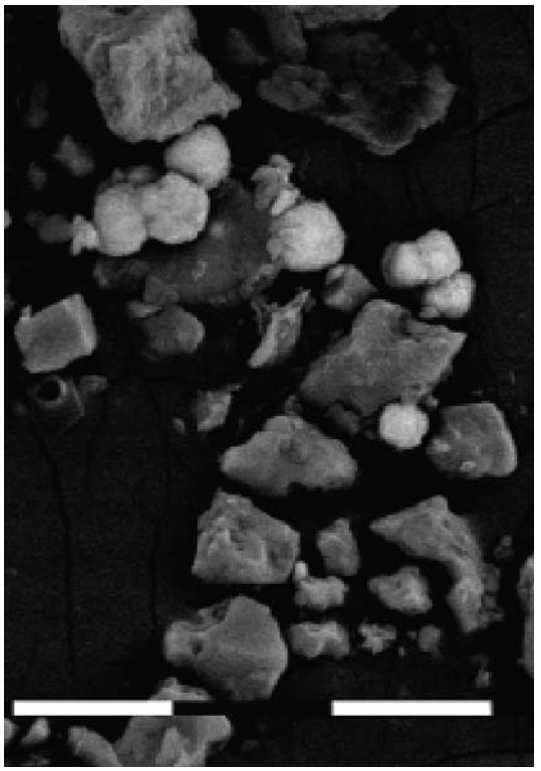

Fig. 13 SEM picture of the Kongressvatnet sediment (scale bar = 10 μm). The light grey spheroidal particles are iron suphides, as confirmed by the high iron and sulphur content in the EDS spectra

IV. Echinenone is totally absent in the topmost 5 cm (zone I). In summary, as inferred from the concentrations of their characteristic carotenoids, siliceous algae (diatom, chrysophytes) and chlorophyceae are the most abundant algal groups in Kongressvatnet, whereas cyanobacteria and truly planktonic algae (alloxanthin; Guilizzoni and Lami 2002) are scarce (Fig. 15).

Photosynthetic purple anaerobic bacteria, as inferred from their specific carotenoids okenone and isorenieratene, are a major component of the microflora of this meromictic lake. The high sulphur content of its waters supports, from 30 cm upwards, two horizontally stratified very abundant populations of photosynthetic bacteria, one near the chemocline (Chromatiaceae) and the other at greater depth (Chlorobiaceae). The photosynthetic pigments of the two groups are distinctive and group-specific. The Chromatiaceae contain the carotenoids okenone (and bacteriochlorophyll *a*), whereas the Chlorobiaceae produce the carotenoid isorenieratene (and bacteriochlorophyll *e*). Compared to some pigments (e.g., fucoxanthin), these carotenoids appear to be less susceptible to diagenesis (Brown et al. 1984; Leavitt 1993). Our data indicate that peaks of okenone concentrations correspond to minimum values of isorenieratene and vice-versa and, consequently, that populations of photosynthetic bacteria have been influenced by water transparency or water turbidity:

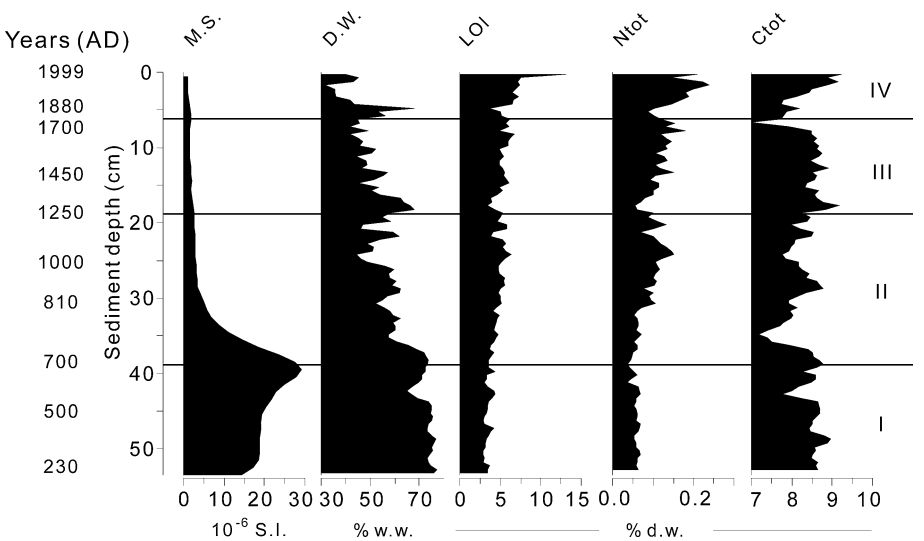

Fig. 14 Selected physical and chemical parameters in core K99-3 of Kongressvatnet. M.S. = magnetic susceptibility; D.W. = dry weight; LOI = Loss on Ignition; Ntot = total nitrogen; Ctot = total carbon

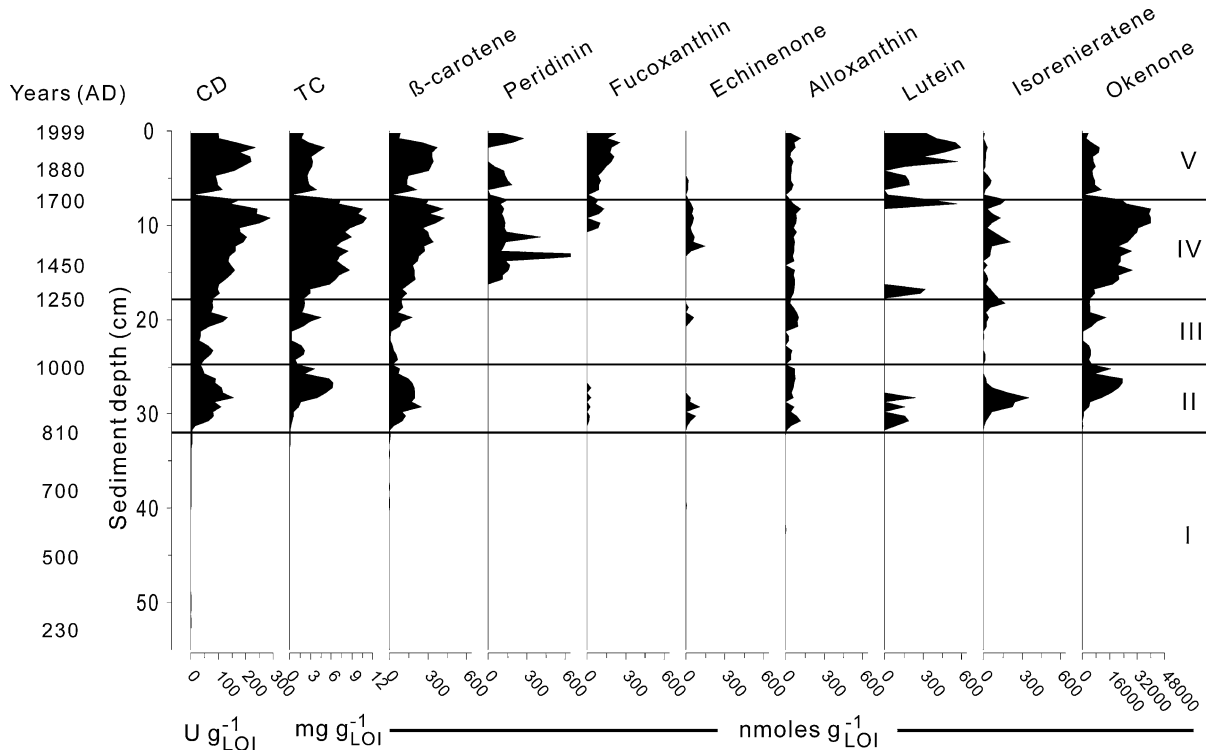

Fig. 15 Total chlorophyll derivatives (CD), total carotenoids (CD) and specific carotenoid concentrations of sediment in core K99-3 from Kongressvatnet

in other words by light availability. Compared with the concentrations of okenone, isorenieratene is, however, very low (Fig. 15). Under reduced light conditions, the Chlorobiaceae, occupying the deepest strata, are most strongly affected. Both populations mark the onset of meromictic conditions of the lake that probably became permanently anoxic and stratified from 18 cm upwards. Deep anoxic conditions were, however, present in earlier periods (zone II). It is difficult to say if these variations in light limitation would affect the algal community as well: compared with the algae, the photosynthetic anaerobic bacteria have a much lower light requirement (they can growth well at very reduced light, $<1\%$ of surface light (Züllig 1985).

The bacteria carotenoids are much more abundant during the LIA (concentrations are very high; zone IV) than warmer periods (e.g., during the Medieval Warm Period (MWP) and recent period; end of zone II and zone III, Fig. 15). The 20th century temperature and climate reconstructions show a clear warming on Svalbard from a study on glacial net mass balance (Lefauconnier and Hagen 1990), yet the bacteria pigments are reduced (zone V). However, from the depth distribution of total pigments (CD, TC and β-carotene), biomass of the algal community is fairly high, indicating that different favourable ambient conditions characterize the 20th century compared with those of the past. Since the concentrations of alloxanthin, a carotenoid that belongs to truly planktonic algae (Guilizzoni and Lami 2002), are very low, no important fluctuations in water level are inferred from its distribution.

Diatoms

A stratigraphic profile of the dominant diatoms is illustrated in Fig. 16. A total of 140 taxa were found, of these 57 had a greater abundance than 1% in any one sample. Specimens of *Cocconeis placentula* and *Fragilaria capucina* were variable and although varieties were initially identified, these were subsequently amalgamated.

The main characteristic of the diatom diagram is that diatoms are absent from the core base up to 18 cm (zone I; ca. AD 1255), when species of

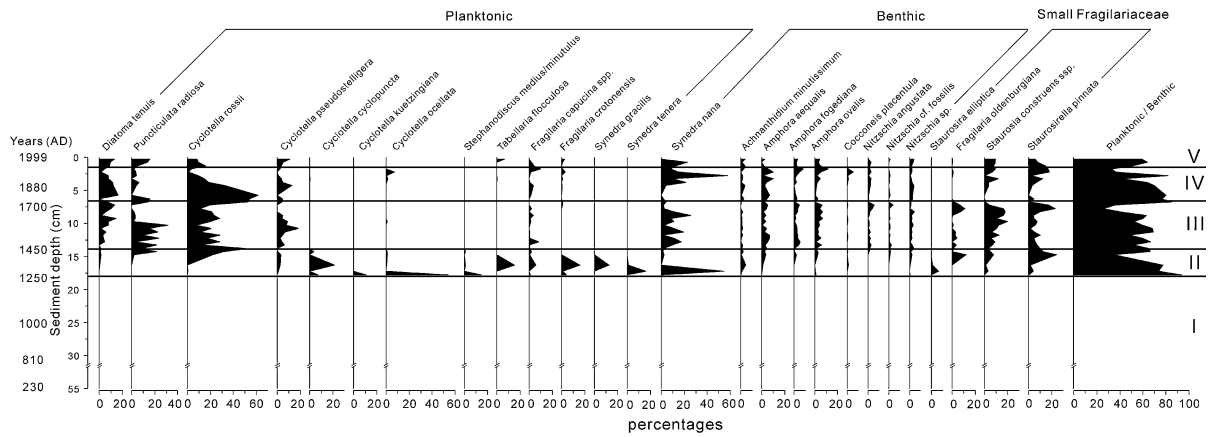

Fig. 16 Relative abundances of major fossil diatom taxa in the sediment core K99-3 from Kongressvatnet

mesotrophic taxa such as *Fragilaria crotonensis*, *Tabellaria flocculosa*, *Synedra tenera* and small *Stephanodiscus* spp. appear (zone II). Two of these species (*F. crotonensis*, *T. flocculosa*) re-appear in low abundance in very recent times (last 40 years). A similar, sudden increase in diatoms in Arctic lakes, although relative to recent times, was also found by Doubleday et al. (1994) and Perren et al. (2003), who explain this event by an environmental change related to the general climatic warming during the last century. Likewise, in Kongressvatnet, diatom appearance at ca. AD 1255 could be explained by an external factor (climatic change) during former times. It is difficult to explain why diatoms when lacking whereas other biological remains such as pigments (although at very low concentrations) and especially Cladocera were not (Fig. 17). We hypothesize that this may be related to the (1) poor preservation in carbonate rich sediment and, (2) extension and duration of ice cover as inferred from the anoxygenic bacteria pigment data which indicate for the deepest part of the core, a long period of ice cover, during which the scarcity of light and nutrients would have prevented extensive algal growth.

From 17 cm upward, the main taxa are typical of oligotrophic water and the community is dominated by the planktonic species, in particular *Cyclotella rossii* that shows several changes in its abundance reaching the maximum value at the end of 19th century (zone IV; Fig. 16). The amount of planktonic diatoms such as *Cyclotella* spp. in relation to the benthic ones, especially small Fragilariaceae, may give some indication of the length and extent of the ice-cover, water-level fluctuation, and the availability of light and nutrients: the longer the ice cover the shorter the growing season for the planktonic diatoms (Smol 1988; Lim et al. 2001). *Fragilaria* species are *r*-strategists, well adapted to changing environmental conditions. Therefore *Fragilaria*-dominated assemblages are common in physically disturbed, unstable environments often characteristic of the early Holocene and recently deglaciated sites (Bradshaw et al. 2000).

In Kongressvatnet, small Fragilariaceae such as *Staurosira construens* and *Staurosirella pinnata*, are never the dominant taxa and their stratigraphic profile shows strong oscillations in general in opposition to the main *C. rossii* trend. Zone III corresponds to a phase of lower percentages of planktonic diatoms and of an increasing abundance of *S. construens*. We believe this represents the LIA with the typical *S. construens/S. pinnata* complex dominating colder, more oligotrophic waters and lower water level (Douglas et al. 1994; Bradshaw et al. 2000; Perren et al. 2003). Fluctuations in water level can be inferred from the planktonic/benthic ratio: several minima values and thus lower water levels are shown during the last century (1.75, 3.25 cm) and during the LIA (between 7.75 and 15.75 cm) core depths.

To verify the above hypothesis, we compared the diatom percentages with the concentrations of fossil pigments. The decrease of planktonic diatom communities is associated with high concentrations of bacterial pigments (isorenieratene and okenone) and a low content of lutein and chlorophyll derivatives. We consider this pigment composition typical of cold

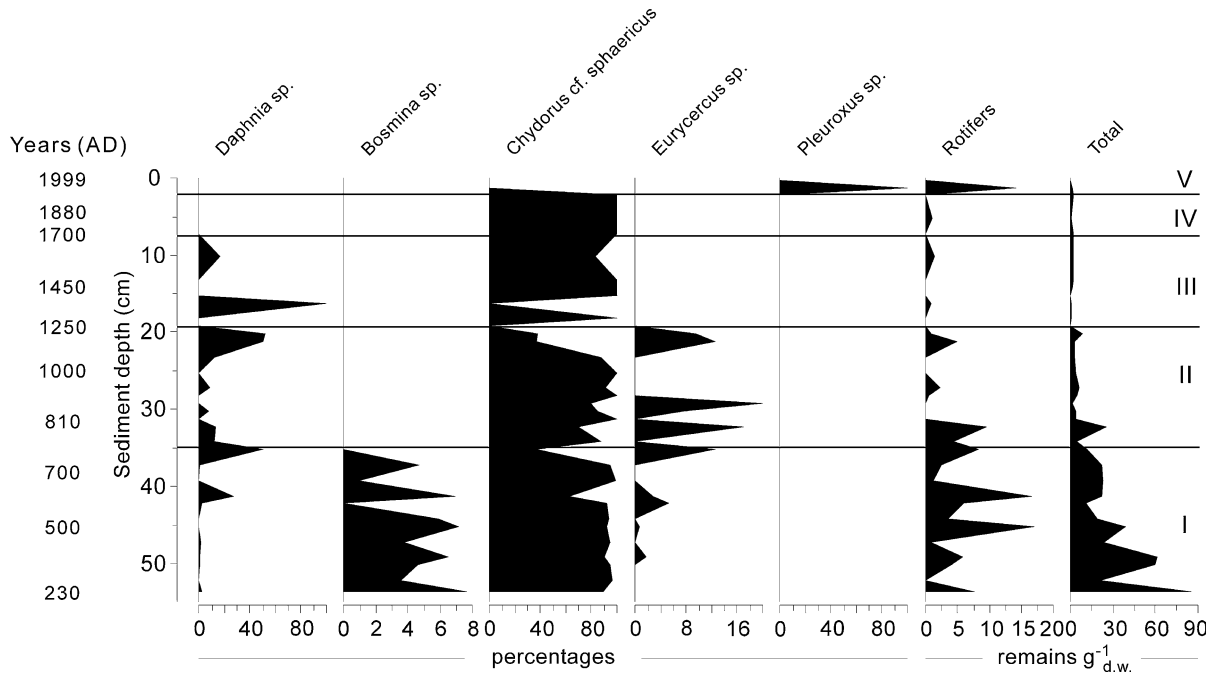

Fig. 17 Distribution of Cladocera and rotifer resting eggs in the sediment core K99-3 from Kongressvatnet

periods, with little vegetation in the watershed contributing lutein and chlorophylls, and a long ice-cover leading to anoxic water. As reported by Overpeck et al. (1997), from mid-1800 to the mid-20th century, the arctic warmed to the highest temperatures in four centuries. This warming marked the end of the LIA and in Kongressvatnet it is marked by a new increase of *Cyclotella* spp. and large benthic diatom species (such as *Diatoma tenuis*) that reach their highest percentages close to the end of 19th century (zone IV). At the same time there is a collapse of *S. construens* and a re-appearance of *F. crotonensis* favoured by an increase in nutrient and silica concentrations following snowmelt.

During the 20th century, the planktonic vs benthic diatom profile shows strong fluctuations (end of zone IV and V), with minima in the percentage of planktonic remains at 3.25 and 1.75 cm depths, indicating extensive ice coverage. On the basis of the ^{210}Pb chronology, these sections are dated 1930 ± 8 and 1969 ± 3, respectively. These dates correspond to two of the three coldest periods of the last century (Isaksson et al. 2001; van de Wal et al. 2002; Perren et al. 2003). A similar decrease in planktonic species abundance is detected at 7.75 cm depth, corresponding to the cold period during the first half of the 18th century. During the 1980s and 1990s (zone V) global temperatures rose to the highest values of the last century, but at Svalbard temperature values have been approximately the same as in the 1920s and lower than during the 1930s and 1950s (Hanssen-Bauer and Førland 1998; Nordli and Kohler 2003); accordingly the fluctuations of planktonic vs benthic ratios follow this climatic changes (Fig. 16).

Cladocera fossil remains and rotifer resting eggs

The concentration of Cladocera subfossil remains in core K99-3 was relatively high in the deeper sections (54–35 cm; zone I; AD 230–756), followed by a gradual decrease, toward the lower values of zone II (AD 756–1250) and the depletion (<1 exuviae g d.w.$^{-1}$) of zones III-V (AD 1250-present), with no remains at 19–19.5 cm level (Fig. 17).

As typically observed in these extreme environments, the Cladocera assemblage is low in species diversity. Among the Chydorids, *Chydorus* cf. *sphaericus* is dominant; quite abundant are a *Eurycercus* species with peaks of relative abundance in zones I and II, and a *Pleuroxus* sp., which is the only Cladocera found in the upper 2 cm sections of the core. Zooplanktonic Cladocera were represented by a

Hyalodaphnia (according to literature information, *D. longispina* or *D. umbra*; Schwenk et al. 2004) and two species of the genus *Bosmina* (largely *Eubosmina. longispina*, except for section 50.5–50 cm, in which *Bosmina longirostris* was found).

The core was characterized by a dominance of *Chydorus*, particularly at depth. This species represented ca. 90% of the total concentration of remains between 54 and 42.5 cm (zone I), in which the second most abundant taxon was *Bosmina* (mainly *Eubosmina*). From 35 cm to the upper part of the core, *Daphnia* replaced *Bosmina* as the second most important genus, and apart from the first cm, in which Cladocera were very few, more than 80% of the Cladocera assemblage was made up by *C*. cf. *sphaericus* and *Daphnia*.

While in zone I *Chydorus* was approx. 10 ten times more abundant than *Daphnia*, in the upper 35 cm sections their abundance appeared comparable, and at some levels, *Daphnia* was even more common than *Chydorus*. This was largely the result of the sharp decrease in the total concentration of remains.

Anoxic conditions might have influenced *Chydorus* abundance and, as in lakes like Kongressvatnet, it is usually confined to bottom water layers, while *Daphnia longispina* is able to migrate vertically and rotifers, as well as immature stages of copepods, usually inhabit the upper layers. However, *Daphnia* was also at very low levels of population density in the upper three zones of the core.

In addition to the Cladocera, rotifer resting eggs were also recovered; they were more abundant in deep sections (zone I and the lowermost part of zone II), and in the topmost 2 cm sections of the core. Despite the lower level of abundance, their share on the total (Cladocera + rotifers) remains increased in the upper 20 cm of the core, particularly at 22, 16, and 5 cm levels (>50%) because of the depletion in cladocerans (data not shown). In the topmost 3 cm they become important, as a result of their increase in abundance and the almost compete depletion of cladocerans.

According to changes in the abundance of Cladocera, we can distinguish two main phases: the first, which is represented by zone I, is characterized by a relatively high concentration of remains, and the second, more recent (zones II-V), in which the concentration of remains was about ten times lower. The assemblage from 54 to 45 cm (Zone I) was characterized by the replacement of *Bosmina*, by a *Hyalodaphnia* species, which at 36 and 22–21 cm levels (Zone II), became even more abundant than the most represented species *C*. cf. *sphaericus*. The presence of *Bosmina* at the base of the core is compatible with the presence of zooplanktivorous fish, as small cladocerans co-occur with fish predation. The shift from *Bosmina* to *Daphnia* represents an increase in mean zooplankton body size, which might be indicative of a decrease in fish predation pressure. On the other hand, pale *D. longispina* are known to be able to coexist with fish predation, contrary to *D. pulex*, which are always depleted in the presence of zooplanktivorous fish (Gliwicz et al. 2001).

A depletion of Cladocera and an increase in relative abundance of rotifers is also consistent with fish predation (Jeppesen et al. 2001; Vadeboncouer et al. 2003). Rotifers, particularly *Polyarthra* sp., dominate arctic lakes (Lauridsen and Hansson 2002). While in temperate lakes Cladocera are an important food for Arctic char, in arctic lakes with fish, they are replaced by copepods, and the latter might have been an important source of the total carotenoids detected in this upper part of the core. This is the case for the upper three zones of the core, in which Cladocera, *Daphnia* included, were almost entirely lacking.

Although chydorids were largely dominant, the increase in the relative abundance of zooplanktonic Cladocera at 42, 35, and 20–21 cm, in which the rotifers share increases, might also be indicative of an increase in water level.

Palaeoenvironmental and palaeoclimate inferences: a synthesis

This study of an arctic lake during the past ca. 1800 years shows five zones of marked environmental changes (Fig. 18). The onset and duration of these changes in core K99-3 (zones I–V) are a balanced integration of the major changes in the proxy-records shown (Figs. 14–17). These changes occurred at ca. AD 700–820; 1160–1255; 1715–1880; 1940–1963s (at ca. 38–32, 20–18, 8–4.5, and 3–2 cm, respectively).

The remoteness of the region means that temporal variations in the limnological conditions of the lakes must be associated with climate changes in the area (Douglas et al. 2000; Birks et al. 2004a). The climatic factors such as those related to the MWP and

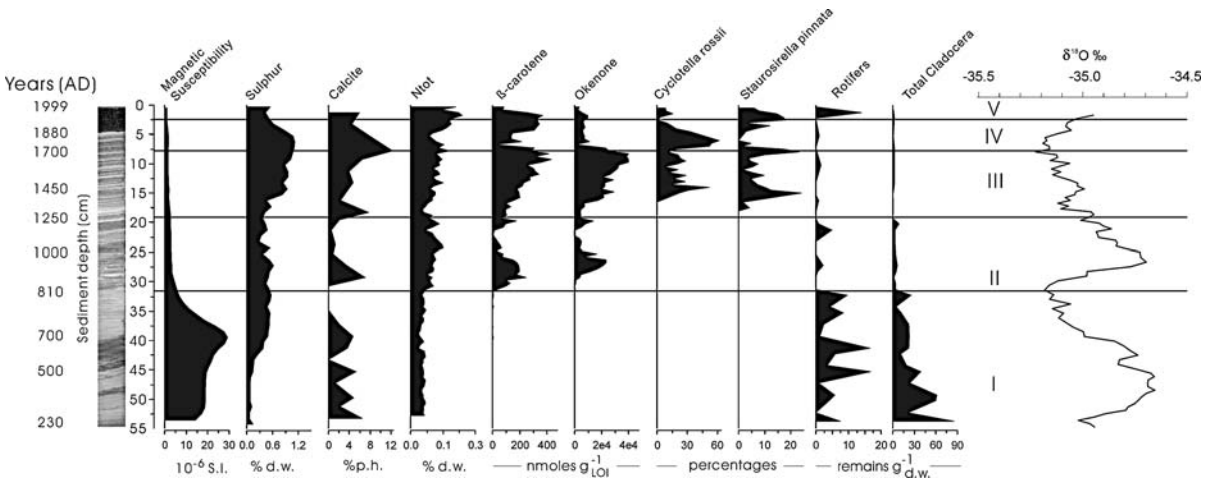

Fig. 18 Summary diagram of multi-proxy records of sediment core K99-3 from Kongressvatnet. A profile on $\delta^{18}O$ record in the GISP2 ice core from Greenland is also shown for comparison (http://www.gisp2.sr.unh.edu/GISP2)

the LIA both represented in our cores (zones II and III), are closely linked to the extent of lake ice-cover that, in turn, determined habitats for biological growth. Regional and local disturbances might be important for some changes during 19th and 20th centuries as shown by some chemical data (LOI, sulphur and nitrogen; Fig. 14) (as also found in other lakes; Birks et al. 2004b). Kongressvatnet is close to mining areas and it is known that in the last century local air pollution, as well as long-range atmospheric transport of pollutants, has been superimposed on climate variability in forcing observed ecosystem fluctuations (Simões and Zagorodnov 2001). The mining village of Barentsburg is very close to the investigated lake and certainly has had an impact (although quite limited) on the lake as shown by the relatively high concentration of carbonaceous particles in a nearby lake (Rose et al. 2004).

The chemical features of the Kongressvatnet sediments display the carbonate signature. The profile of S is characterized upwards by a sharp increase in S content and this enrichment could be related to a higher sulphide content: many spheroidal particles of iron suphides were found (Fig. 13).

The topmost 3–4.5 cm layer (zone V) (thickness depending on core positions; Fig. 3) composed by black organic-rich material (LOI of 7–13% d.w.) has been dated in core K99-3 by ^{210}Pb as AD 1880–1999. From the inspections of aerial photographs taken in August 1969 (S69 2481, S69 2482, S69 2483, Norwegian Polar Institute), it seems that at some stage the glacier front retreated so far back that the melt water no longer drained into the lake and thus the upper part of organic sediment might be a result of soil erosion and influx of soil organic matter. Weathering of nutrients and a longer growing season due to warming can also enhance in-lake production. The increase of autochthonous production could also be the result of a less turbid water column from decreased glacial meltwater input. This confirms earlier reports based on geochemical data from 23 Svalbard lakes (Birks et al. 2004b). The recent increase of sedimentation rates (from 1963 up to the present; Fig. 8), the lithological change and a general increase in production of almost all the biological records may be due to an increase in temperature and winter precipitation by 29%, as recorded at the Ny-Ålesund meteorological station (Lefauconnier and Hagen 1990). This corroborates ice core data from Svalbard indicating that rapid warming took place from about the end of the 1800s and during the last 40 years, with a cold phase from 1930 to 1960 (Isaksson et al. 2003).

The uppermost 32 cm of the record (zones II–V; Fig. 18) are characterized by laminated sediments, a low magnetic susceptibility, low magnetic mineral content, higher water content of 60–80%, S sulphides, abundance of algal and bacterial pigments and diatoms (from 18 cm upward), and low concentrations of Cladocera. The peak in magnetic susceptibility at the 38 cm horizon (AD 700) marks two different sediment sources for the magnetic supply as

a possible consequence of meltwater or glacier emplacement occurring in the catchment area. The subsequent decline occurred in a period of rapid cooling (Jansen and Koç 2000) (Fig. 18). In zone I, grain size significantly increases, which could be an explanation for the lower H_2O contents which would have been affected by the fine sandy layers.

From the end of zone I upward a strong oxygen depletion was established in the deep water, of the lake, as inferred from the high concentrations of specific carotenoids from sulphur photosynthetic bacteria (Fig. 15). Changes in elemental composition might be due to changes in the source region because most of the sediment is of detrital origin. Two major rivulets, one formerly from the glacier and one slightly west, run through different bedrock and could have changed their course through time. Such changes in sediment source can be induced by changes in the catchment configuration through glacier activity (Bennet et al. 1999). Such activity might have also dammed the rivulets which presently bring sulphur into the lake. Variable carbonates/silicates and calcite/dolomite ratios occur throughout the core and this suggests changing sediment supply through time (Fig. 11). Oxic conditions and allochthonous input during the earlier part of the record (54.5–38 cm) might also explain the higher susceptibility values because dissolution of magnetic particles is reduced under less anoxic conditions.

The coarser grain sizes in combination with the more frequent sandy event layers in zone I (cf. Fig. 3) clearly indicates a higher energy deposition mode. This could be either related to summer rains on deeper thawed permafrost or to stronger glacial melt water fluxes from a glacier closer to the coring site (more proximal position).

The bi-partition of the clastic part of the Kongressvatnet sediments with a gradual transition between 38 and 18 cm (core K99-3; zone II) is well expressed in the appearance of varves only in the upper part (Figs. 3 and 5). Thus, a change in the limnological state of the lake with favourable conditions for varve formation is inferred, which probably reflects the transition from the Medieval Warm Period to the LIA in this region. Varve preservation is favoured by chemical stratification of the lake indicating meromictic conditions (vertical water circulation does not extend to the bottom of water column). The development of meromixis is coincident with high concentrations of carotenoids (okenone and isorenieratene) of strictly anaerobic sulphur photosynthetic bacteria (zones II–III, Figs. 15 and 18). The hypolimnion of the lake became anoxic because of salty input from streams (Bøyum and Kjensmo 1970) and climate deterioration (longer ice cover periods). Marine water influx can be excluded as cause for meromictic conditions (Svendsen et al. 1987). Stable meromictic conditions were established from ca. AD 1370–1400 (onset of LIA) when varves became continuously preserved.

Prior to the 8th century extremely low algal pigments were detected as well as fossil diatoms (Figs. 15, 16, 18: zone I). This was probably caused by shorter ice cover and resulting longer periods of water circulation. Higher water turbulence, associated with high turbidity, are supported by the coarser grained sediments representing higher energy deposition modes. In contrast to the phytoplankton community, relatively abundant Cladocera remains (mainly *Chydorus* spp.) were found in this oldest part of the core (Figs. 17, 18). Anoxic conditions might have influenced such an abundance from approx. 32 cm upward, as *Chydorus* spp. are confined to the littoral zone.

The continuous presence of varves between AD 1350–1880 (zone III; Figs. 3 and 18) could be likely associated with the presence of glaciers in the catchment of Lake Kongressvatnet during the LIA and related meltwater input (Svendsen and Mangerud 1987) in combination with longer periods of lake freezing in winter. Thus, the main period of glacier advance lasted for about five centuries. In particular, thicker varves in the early part of LIA are likely associated with relatively warm summers, which might be related to a more continental climate as reported for northern Europe (Jones and Bradley 1992). Lower summer temperatures between AD 1800 and 1850 are indicated by thin varves (reduced summer snow-melt). Following this interpretation the coldest summers occurred between AD 1815–1817 (Fig. 6) when the eruption of Tambora affected the short-term global climate.

In conclusion, this study, using many sources of proxy data, has shown that Kongressvatnet has undergone significant environmental and climatic changes during the last 1800 years. The Dark Age Cold Period (zone I), the MWP (base of zone II) as well as the LIA (LIA; zone III) had major environ-

mental impacts on the biological and geochemical lake evolution. Compared to central Europe, a rather earlier onset and later end of LIA (ca. AD 1350 and 1880, respectively) is shown, which correlates well with ice-core studies from Svalbard (Isaksson et al. 2001, 2003) and the GISP2 Greenland ice core (Fig. 18). The sedimentation rates and increase in LOI during the past 40 years were similar to those found elsewhere on Svalbard (unpublished data; Birks et al. 2004b) and in other studies in the Canadian and Finnish Arctic (Smol et al. 2005). All of these studies interpreted the changes as responses to climate changes. The general significance of this study lies in the documentation of the sensitivity of this Arctic lake to environmental change, the qualitative documentation of a high level of climatically forced variability in the late Holocene and the detailed analysis of this variability which includes elements that are comparable with the GISP2 ice core. However, since there is very limited knowledge of high arctic limnological and sedimentary processes, further studies of a complex of factors including catchment geology, morphology and aeolian process are necessary to investigate the source and/or the processes leading to these changes. This is particularly important in view of the fact that Svalbard lakes are environmentally and biologically diverse (Birks et al. 2004b).

Acknowledgements This paper is a contribution to the CNR-POLARNET Strategic Programme. CNR partially supported the field campaign. We would like to thank Stefano Poli, Gabriele Tartari and Roberto Sparapani for their help during field work and logistic assistance. A. Werner supplied us with the photo shown in Fig. 2 and general information on the glaciers. Thanks are due to Timo Saarinen for providing us with palaeomagnetic data of the Finnish lake reported in Fig. 9. Many thanks are due to H.J.B. Birks, Frank Oldfield, Mike Adams and two reviewers (J. Mangerud and an anonymous reviewer) for the constructive comments which were most helpful in improving the manuscript. The authors wish to thank the Norwegian Polar Institute for permission to reproduce the aerial photo shown in Fig. 2.

References

Anderson NJ (2000) Diatoms, temperature and climate change. Eur J Phycol 35:307–314

Andreev AA, Tarasov PE, Siegert C, Ebel T, Klimanov VA, Melles M, Bobrov AA, Dereviagin A Yu, Lubinski DJ, Hubberten HW (2003) Late Pleistocene and Holocene vegetation and climate on the northern Taymyr Peninsula, Arctic Russia. Boreas 32(3):484–505

Andreev AA, Tarasov PE, Klimanov VA, Melles M, Lisitsyna OM, Hubberten HW (2004) Vegetation and climate changes around the Lama Lake, Taymyr Peninsula, Russia during the Late Pleistocene and Holocene. Quater Intl 122:69–85

Antoniades D, Douglas MSV, Smol JP (2005) Quantitative estimates of recent environmental changes in the Canadian High Arctic inferred from diatom in lake and pond sediments. J Paleolimnol 33:349–360

Appleby PG (2004) Environmental change and atmospheric contamination on Svalbard: sediment chronology. J Paleolimnol 31:433–443

Appleby PG, Oldfield F (1978) The calculation of ^{210}Pb dates assuming a constant rate of supply of unsupported ^{210}Pb to the sediment. Catena 5:1–18

Appleby PG, Oldfield F (1983) The assessment of ^{210}Pb data from sites with varying sediment accumulation rates. Hydrobiologia 103:29–35

Battarbee RW (2000) Palaeolimnological approaches to climate change, with special regard to the biological record. Quat Sci Rev 19:107–124

Bennet MR, Hambrey MJ, Huddart D, Glasser NF, Crawford K (1999) The landform and sediment assemblage produced by a tidewater glacier surge in Kongsfjorden, Svalbard. Quat Sci Rev 18:1231–1246

Berglund BE (2003) Human impact and climate changes—synchronous events and a casual link? Quater Intl 105:7–12

Berner RA (1970) Sedimentary pyrite formation. Am J Sci 268:1–23

Birks HH (1991) Holocene vegetational history and climatic change in west Spitsbergen—plant macrofossil from Skardtjørna, an Arctic lake. The Holocene 1:209–215

Birks HJB, Jones VJ, Rose NL (2004a) Recent Environmental change and atmospheric contamination on Svalbard as recorded in lake sediments – an introduction. J Paleolimnol 31:403–410

Birks HJB, Jones VJ, Rose NL (2004b) Recent Environmental change and atmospheric contamination on Svalbard as recorded in lake sediments – synthesis and general conclusions. J Paleolimnol 31:531–546

Bøyum A, Kjensmo J (1970) Kongressvatnet. A crenogenic meromictic lake at Western Spitsbergen. Arch Hydrobiol 67:542–552

Bøyum A, Kjensmo J (1980) Post-Glacial sediments in Lake Linnévatn, Spitsbergen. Arch Hydrobiol 88:232–249

Bradshaw EG, Jones VJ, Birks HJB Birks HH (2000) Diatom responses to late-glacial and early-Holocene environmental changes at Kråkenes, western Norway. J Paleolimnol 23:21–34

Brauer A (2004) Annually laminated lake sediments and their palaeoclimatic relevance. In: Fischer H, Kumke T, Lohmann G, Flöser G, Miller H, von Storch H, Negendank JFW (eds) The climate in Historical times. Towards a synthesis of Holocene proxy data and climate models. Springer, Berlin, pp. 109–128

Brauer A, Hajdas I, Negendank JFW, Vos H, Rein B, Zolitschka B (1994) Warvenchronologie. Eine Methode zur absoluten Datierung und Rekonstruktion kurzer und mittlerer solarer Periodizitäten. Geowissenschaften 12:325–332

Briffa KR, Schweingruber FH, Jones PD, Osborn TJ, Shiyatov SG, Vaganov EA (1998) Reduced sensitivity of recent tree-growth to temperature at high northern latitudes. Nature 391:678–682

Brown SR, McIntosh HJ, Smol JP (1984) Recent paleolimnology of a meromictic lake: fossil pigments of photosynthetic bacteria. Verh Int Ver Limnol 22:1357–1360

Dallmann WK (ed) (1993) Geological map of Svalbard 1:500,000, sheet 1G, Spitsbergen, southern part, Sheet 3G, northern part. Preliminary edition. Norsk Polarinstitutt

Daly L, Le Goff M (1996) An updated and homogeneous world secular data base. 1. Smoothing of the archeomagnetic results. Phys Earth Planet Int 93:159–190

Doubleday NC, Douglas MSV, Smol JP (1995) Paleoenvironmental perspectives on black carbon deposition in the high Arctic. Sci Total Envir 160(161):661–668

Douglas MSV, Smol JP, Blake W (1994) Marked post-18th century environmental change in high-arctic ecosystems. Science 266:416–419

Douglas MSV, Smol JP, Blake W Jr (2000) Summary of palaeolimnological investigations of High Arctic ponds at Cape Herschel, east-central Ellesmere Island, Nunavut. In: Garneau M, Alt BT (eds) Environmental response to Climate Change in the Canadian high Arctic. Geol Surv Can Bull 529:257–269

Dypvik H, Harris NB (2001) Geochemical *facies* analysis of fine grained siliciclastic using Th/U, Zr/Rb and (Zr+Rb)/Sr ratios. Chem Geol 181:131–146

Franzini M, Leoni L, Saitta M (1972) A simple method to evaluate the matrix effects in X-ray fluorescence analysis. X-ray Spectrom 1:151–154

Franzini M, Leoni L, Saitta M (1975) Revisione di una metodologia analitica per fluorescenza-X basata sulla correzione completa degli effetti di matrice. Rend Soc ital Mineral Petrol 31:365–378

Frey DG (1958) The Late-Glacial cladoceran fauna of a small lake. Arch Hydrobiol 54:209–275

Frey DG (1986) Cladocera analysis. In: Berglund BE (ed) Handbook of Holocene palaeoecology and palaeohydrology. Wiley J and Sons, pp 667–692

Frignani M, Langone L, Ravaioli M, Sticchi A (1991) Cronologia di sedimenti marini. Analisi di radionuclidi naturali ed artificiali mediante spettromentria gamma. IGM-CNR Technical Report no. 24:32 pp

Giordani P, Hammond DE, Berelson WM, Montanari G, Poletti R, Milandri A, Frignani M, Langone L, Ravaioli M, Rovatti G, Rabbi E (1992) Benthic fluxes and nutrient budgets for sediments in the Northern Adriatic Sea: burial and recycling efficiencies. Sci Total Environ (Suppl 1992):251–275

Gliwicz Z, Slusarczyk MA, Slusarczyk M (2001) Life history synchronization in a long-lifespan single-cohort *Daphnia* population in a fishless alpine lake. Oecologia 128:368–378

Grootes PM, Stuiver M, White JWC, Johnsen SJ, Jouzel J (1993) Comparison of oxygen isotope records from the GISP2 and GRIP Greenland ice cores. Nature 366:552–554

Guilizzoni P, Lami A (2002) Palaeolimnology: use of algal pigments as indicators. In: Bitton G (ed) The encyclopedia of environmental microbiology. Wiley and Sons, pp 2306–2317

Hann BJ, Karrow PF (1993) Comparative analysis of cladoceran microfossils in the Don Scarborough formation, Toronto, Canada. J Paleolimnol 9:223–241

Hanssen-Bauer I, Førland EJ (1998) Long-term in precipitation and temperature in the Norwegian Arctic: can they be explained by changes in atmospheric circulation patterns? Clim Res 10:143–153

Hardy DR, Braun C, Bradley RS, Retelle MJ (1998) The climate signal within clastic lake sediments, Canadian High Arctic. Paleo Times, The Paleoclimates from Arctic Lakes and Estuaries Newsletter 6:34

Hofmann W (1978) Analysis of animal microfossils from the Grosser Segerberger See (F.F.G.). Arch Hydrobiol 82:316–346

Isaksson E, Pohjola V, Jauhiainen T, Moore J, Pinglot JF, Vaikmae R, Van De Wal RSW, Hagen JO, Ivask J, Karlof L, Martma T, Meijer HAJ, Mulvaney R, Thomassen M, Van Den Broeke M (2001) A new ice, core record from Lomonosovfonna, Svalbard: Viewing the 1920–97 data in relation to present climate and environmental conditions. J Glaciol 47(157):335–345

Isaksson E, Hermanson M, Hicks S, Igarashi M, Kamiyama K, Moore J, Motoyama H, Muir D, Pohjola V, Vaikmae R, van de Wal RSW, Watanabe O (2003) Ice cores from Svalbard—useful archives of past climate and pollution history. Phys Chem Earth 28(28–32):1217–1228

Jansen E, Koç N (2000) Century to decadal scale records of Norwegian sea surface variations of the past 2 millennia. PAGES Newslet 8:13–14

Jeppesen E, Christoffersen K, Landkildehus F, Lauridsen T, Amsinck S (2001) Fish and crustaceans in northeast Greenland lakes with special emphasis on interactions between Arctic charr (*Salvelinus alpinus*), *Lepidurus arcticus* and benthic chydorids. Hydrobiologia 442:329–337

Jones PD, Bradley RS (1992) Climatic variations over the last 500 years. In: Bradley RS, Jones PD (eds) Climate since A.D. 1500, Routledge, London, pp 649–665

Jones B, Manning DAC (1994) Comparison of geochemical indices used for the interpretation of palaeo-redox conditions in ancient mudstones. Chem Geol 111:111–129

Karst-Riddoch TL, Pisaric MFJ, Smol J.P (2005) Diatom responses to 20th century climate-related environmental changes in high-elevation mountain lakes of the northern Canadian Cordillera. J Paleolimnol 33:265–282

Korhola A, Tikkanen M, Weckström J (2005) Quantification of Holocene lake-level changes in Finnish Lapland using a Cladocera-lake depth transfer model. J Paleolimnol 34:175–190

Krammer K, Lange-Bertalot H (1986–1991) Süsswasserflora von Mitteleuropa, Band 2, Teil 1–4. Gustav Fischer Verlag. Stuttgart, pp 876 + 596 + 576 + 436

Kremenetski KV, Boettger T, MacDonald GM, Vaschalova T, Sulerzhitsky L, Hiller A (2004) Medieval climate warming and aridity as indicated by multiproxy evidence from the Kola Peninsula, Russia. Palaeogeogr Palaeoclimatol Palaeoecol 209:113–125

Lami A, Guilizzoni P, Marchetto A (2000b) High resolution analysis of fossil pigments, carbon, nitrogen and sulphur in the sediment of eight European Alpine lakes: the MOLAR project. J Limnol 59(Suppl 1):15–28

Lami A, Korhola A, Cameron N (eds) (2000a) Paleolimnology, climate variability and ecosystem dynamics at remote European alpine lakes (Mountain Lakes Research programme, MOLAR). J Limnol 59 (Suppl 1):119

Lami A, Niessen F, Guilizzoni P, Massaferro J, Belis C (1994) Palaeolimnological studies of the eutrophication of volcanic Lake Albano (Central Italy). J Paleolimnol 10:181–197

Lauridsen T, Hansson LA (2002) The zooplankton community of five Faroese lakes. Ann Soc Sci Færoensis Suppl 36:70–78. Distribution of the species. Medd. Grønland 180:1–249

Leavitt PR (1993) A review of factors that regulate carotenoid and chlorophyll deposition and fossil pigment abundance. J Paleolimnol 9:109–127

Leavitt PR, Hodgson DA (2001) Sedimentary pigments. In: Smol JP, Birks HJB, Last WM (eds) Tracking environmental change using lake sediments, Vol 3: terrestrial, algal, and siliceous indicators. Kluwer academic Publisher, Dordrecht, The Netherlands

Leemann A, Niessen F (1994) Varve formation and the climatic record in an Alpine proglacial lake: calibrating annually-laminated sediments against hydrological and meteorological data. The Holocene 4:1–8

Lefauconnier B, Hagen JO (1990) Glaciers and climate in Svalbard: statistical analysis and reconstruction of the Brøggerbreen mass balance for the last 77 years. Ann Glaciol 14:148–152

Leoni L, Saitta M (1976) X-ray fluorescence analysis of 29 trace elements in rock and mineral standards. Rend Soc ital Mineral Petrol 32:497–510

Leoni L, Menichini M Saitta M (1982) Determination of S, Cl and F in silicate rocks by X-ray fluorescence analyses. X-Ray Spectrom 11:56–158

Lim DSS, Douglas MSV, Smol JP (2001) Diatoms and their relationship to environmental variables from lakes and ponds on Bathurst Island, Nunavut, Canadian High Arctic. Hydrobiologia 450:215–230

Lotter A, Heiri O, Tinner W (2002) Climate reconstructions from lake sediments in the Alpine region. ESF-HOLIVAR workshop, Lammi, Finland, April 17–20th, 2002, Discussion Paper, 4 pp

Løvlie R, Svendsen JI, Mangerud J (1991) High-latitude Holocene paleosecular variation and magneto-stratigraphic correlation between two lakes on Spitsbergen (78° N). Physics of the Earth and Planetary Interior 67:348–361

Musazzi S (2005) Evoluzione del paleoambiente e del paleoclima del tardo Olocene in due aree remote (Svalbard e Himalaya) attraverso l'analisi di sedimenti lacustri. PhD Thesis, University of Parma, 157 pp

Nowaczyk NR, Harwart S, Melles M (2001) Impact of early diagenesis and bulk particle grain size distribution on estimates of relative geomagnetic palaeointensity variations in sediments from Lama Lake, Northern Central Siberia. Geophys J Intl 145(1):300–306

Nordli Ø, Kohler J (2003) The early 20th century warming: Daily observations at Green Harbour, Grønfjorden, Spitsbergen. Norwegian Meteorological Institute. Report Klima 12(03):20

Overpeck J, Hughen K, Hardy D, Bradley R, Case R, Douglas M, Finney B, Gajewski K, Jacoby G, Jennings A, Lamoureux S, Lasca A, MacDonald G, Moore J, Retelle M, Smith S, Wolfe A, Zielinski G (1997) Arctic Environmental change of the last four centuries. Science 278:1251–1256

Perren BB, Bradley RS, Francus P (2003) Rapid Lacustrine Response to Recent High Arctic Warming: A Diatom Record from Sawtooth Lake, Ellesmere Island, Nunavut. Arctic, Antarctic Alpine Res 35:271–278

Pielou EC (1977) Mathematical ecology. J Wiley and Sons, NY, pp 385

Pinglot JF, Pourchet M, Lefauconnier B, Hagen JO, Isaksson E, Vaikmäe R, Kamiyama K (1999) Accumulation in Svalbard glaciers deduced from ice cores with nuclear tests and Chernobyl reference layers. Polar Res 18:315–321

Pourchet M, Lefauconnier B, Pinglot JF, Hagen JO (1995) Mean net accumulation of ten glacier basins in Svalbard estimated from detection of radioactive layers in shallow ice cores. Zeitschrift für Gletscherkunde und Glazialgeologie 31:73–84

Rahn KA (eds) (1981) Arctic air chemistry. Atmos Environ 15:1345–1516

Renberg I (1990) A procedure for preparing large sets of diatom slides from sediment cores. J Paleolimnol 4:87–90

Rose NL, Rose CL, Boyle JF, Appleby PG (2004) Lake sediment evidence for local and remote sources of atmospherically deposited pollutants on Svalbard. J Paleolimnol 31:499–513

Saarinen T (1999) Palaeomagnetic dating of Late Holocene sediments in Fennoscandia. Quat Sci Rev 18:889–897

Santisteban JI, Mediavilla R, López-Pamo E, Dabrio CJ, Zapata MBR, García MJG, Castaño S, Martínez-Alfaro PE (2004) Loss on ignition: a qualitative or quantitative method for organic matter and carbonate mineral content in sediments? J Paleolimnol 32:287–299

Schwenk K, Junttila P, Rauttio M, Bastinasen F, Knapp J, Dove O, Billiones R, Streit B (2004) Ecological, morphological and genetic differentiation of *Daphnia* (*Hyalodaphnia*) from the Finnish and Russian subarctic. Limnol Oceanogr 49:532–539

Simões JC, Zagorodnov VS (2001) The record of anthropogenic pollution in snow and ice in Svalbard, Norway. Atmos Environ 35:403–413

Smith SV, Bradley RS, Abbott MB (2004) A 300 year record of environmental change from Lake Tuborg, Ellesmere Island, Nunavut, Canada. J Paleolimnol 32:137–148

Smol JP (1988) Paleoclimate proxy data from freshwater arctic diatoms. Verh Internat Verein Limnol 23:837–844

Smol JP, Walker IR, Leavitt PR (1991) Paleolimnology and hindcasting climatic trends. Ver Int Ver Limnol 24:1240–1246

Smol JP (and other 25 co-authors) (2005) Climate-driven regime shifts in the biological communities of arctic lakes. Proc Nat Acad Sci 102:4397–4402

Snowball IF (1991) Magnetic hysteresis properties of greigite (Fe_3S_4) and a new occurence in Holocene sediments from Swedish Lappland. Phys Earth Planet Inter 68:32–40

Snyder JA, Miller GH, Werner A, Jull AJT, Stafford Jr TW (1994) AMS-radiocarbon dating of organic-poor lake sediment, an example from Linnévatnet, Spitsbergen, Svalbard. The Holocene 4:413–421

Svendsen JI, Mangerud J (1997) Holocene glacial and climatic variations on Spitsbergen, Svalbard. The Holocene 7:45–57

Svendsen JI, Landvik JY, Mangerud J, Miller GH (1987) Postglacial marine and lacustrine sediments in Lake Linnévatnet, Svalbard. Polar Res 5:281–283

Thouveny N, Williamson D (1991) Paleomagnetic secular variation as a chronological tool for the Holocene. In: Frenzel B, Pons A, Glaeser B (eds) Evaluation of climate proxy data in relation to the European Holocene. Special issue: European Science Foundation Project on European palaeoclimate and man. Palaeoklimaforschung 6:13–27

Vadeboncouer Y, Jeppesen E, Vander Zanden MJ, Schierup HH, Christoffersen K, Lodge DM (2003) From Greenland to green lakes: cultural eutrophication and the loss of benthic pathways in lakes. Limnol Oceanogr 48:1408–1418

van de Wal RSW, Mulvaney R, Isaksson E, Moore JC, Pinglot JF, Pohjola VA, Thomassen MPA (2002) Reconstruction of the historical temperature trend from measurements in a medium, length borehole on the Lomonosovfonna plateau, Svalbard. Ann Glaciol 35:371–378

Wagner B, Melles M, Hahne J, Niessen F, Hubberten HW (2000) Holocene climate history of Geographical Society Ø, East Greenland—evidence from lake sediments. Palaeogeogr Palaeoclimatol Palaeoecol 160:45–68

Werner A (1993) Holocene moraine chronology, Spitsbergen, Svalbard: lichenometric evidence for multiple Neoglacial advances in the Arctic. The Holocene 3:128–137

Willemse NW, Törnqvist T (1999) Holocene century-scale temperature variability from West Greenland lake records. Geology 27:580–584

Zolitschka B (1996) Image analysis and microscopic investigation of annually laminated lake sediments from Fayetteville Green Lake (NY, USA), Lake C2 (NWT, Canada) and Holzmaar (Germany): a comparison. In: Kemp AES (ed) Palaeoclimatology and Palaeoceanography from laminated sediments, vol. 116, Geological Society of London Special Publication, pp 49–55

Züllig H (1985) Pigmente phototropher Backerien in Seesedimenten und ihre Bedeutung für die Seenforschung (mit Ergebnissen aus dem Lago di Cadagno, Rotsee und Lobsigensee. Schweiz Z Hydrol 47:87–126